

Genesis of the Paleozoic Aqishan-Yamansu arc-basin system and Fe (-Cu) mineralization in the Eastern Tianshan, NW China

Jinsheng Han^a, Huayong Chen^{a,b,*}, Hongjun Jiang^c, Liandang Zhao^d, Weifeng Zhang^e, Chun-Kit Lai^{f,g}

^a Key Laboratory of Mineralogy and Metallogeny, Guangzhou Institute of Geochemistry, Chinese Academy of Sciences, Guangzhou 510640, China

^b State Key Laboratory of Ore Deposit Geochemistry, Institute of Geochemistry, Chinese Academy of Sciences, Guiyang 550002, China

^c Geological Party No. 224, China-Shaanxi Nuclear Industry Group, Xi'an 710100, China

^d School of Earth Science and Resources, Chang'an University, Xi'an 710100, China

^e Wuhan Center of China Geological Survey, Wuhan 430205, China

^f Faculty of Science, Universiti Brunei Darussalam, Gadong BE1410, Brunei Darussalam

^g Centre of Excellence in Ore Deposits (CODES), University of Tasmania, Hobart, Tasmania 7001, Australia

ARTICLE INFO

Keywords:

Aqishan-Yamansu belt
Fe (-Cu) mineralization
External sulfur
Basin inversion
Eastern Tianshan (NW China)

ABSTRACT

The formation of the Eastern Tianshan orogen (northern Xinjiang, NW China) with a number of EW-trending mineralization belts was closely linked to the evolution of the Junggar and South Tianshan oceans, probably part of the Paleo-Asian Ocean. Among these Eastern Tianshan mineralization belts, the Carboniferous Aqishan-Yamansu Fe (-Cu) belt hosts a total reserve of 207 Mt Fe and economic Cu endowments for many deposits. These Fe (-Cu) deposits are hosted in submarine volcanic rocks (Lower Carboniferous Yamansu Formation and Upper Carboniferous Tugutublak Formation) and are featured by the presence of extensive skarn alteration without apparently-causative intrusive rocks, which leads to debates over their genesis. In this paper, we have summarized the ore deposit geology, geochemistry and stable isotopes of the Aqishan-Yamansu Fe (-Cu) deposits and discuss their genesis under the regional tectonic framework. We suggest that the Carboniferous Aqishan-Yamansu belt may have been a forearc basin formed by the south-dipping subduction of the Kangguer Ocean beneath the Central Tianshan massif. The Yamansu Formation volcanic rocks and some syngenetic Fe deposits may have formed during the opening of the forearc basin. The Tugutublak Formation volcanic rocks and most Fe (-Cu) deposits may have formed during the subsequent Late Carboniferous basin inversion. In these Aqishan-Yamansu Fe (-Cu) deposits, the Fe mineralization occurred earlier and was likely formed directly from the magmatic-hydrothermal fluids, whereas the subsequent Cu mineralization was likely caused by the gradual increase of seawater or basinal brine influx into the fluid system (external sulfur). The probable external sulfur input, the absence of clear plutonic link, and the temporal coincidence of peak mineralization and basin inversion for the Carboniferous Aqishan-Yamansu Fe-Cu mineralization are comparable to the Mesozoic IOCG mineralization in the Central Andes.

1. Introduction

The Central Asian Orogenic Belt (CAOB), the world's largest Phanerozoic accretionary orogen, has recorded a long-term and complex evolution history of the Paleo-Asian Ocean (Fig. 1a; Windley et al., 2007; Khain et al., 2003; Xiao et al., 2012, 2015). The Junggar and South Tianshan oceans are widely regarded to have constituted the southern part of the Paleo-Asian Ocean, and their opening and closure have formed the Paleozoic Eastern Tianshan orogen (Xinjiang, NW

China), a key component of the southern CAOB (e.g. Xiao et al., 2012, 2013). The Eastern Tianshan is economically important as it hosts a number of subparallel, EW-trending mineralization belts, notably (from north to south) the Tuwu-Yandong Cu belt, Kangguer Au belt and the Aqishan-Yamansu Fe (-Cu ± Au) belt (Wang et al., 2006; Chen et al., 2012; Wang et al., 2014).

It is generally agreed that the Tuwu-Yandong Cu belt was an island arc (i.e., Dananhu-Tousuquan island arc) whereas the Kangguer Au belt was a ductile shear zone (i.e., Kangguer-Huangshan shear zone)

* Corresponding author at: Key Laboratory of Mineralogy and Metallogeny, Guangzhou Institute of Geochemistry, Chinese Academy of Sciences, Guangzhou 510640, China.

E-mail address: huayongchen@gig.ac.cn (H. Chen).

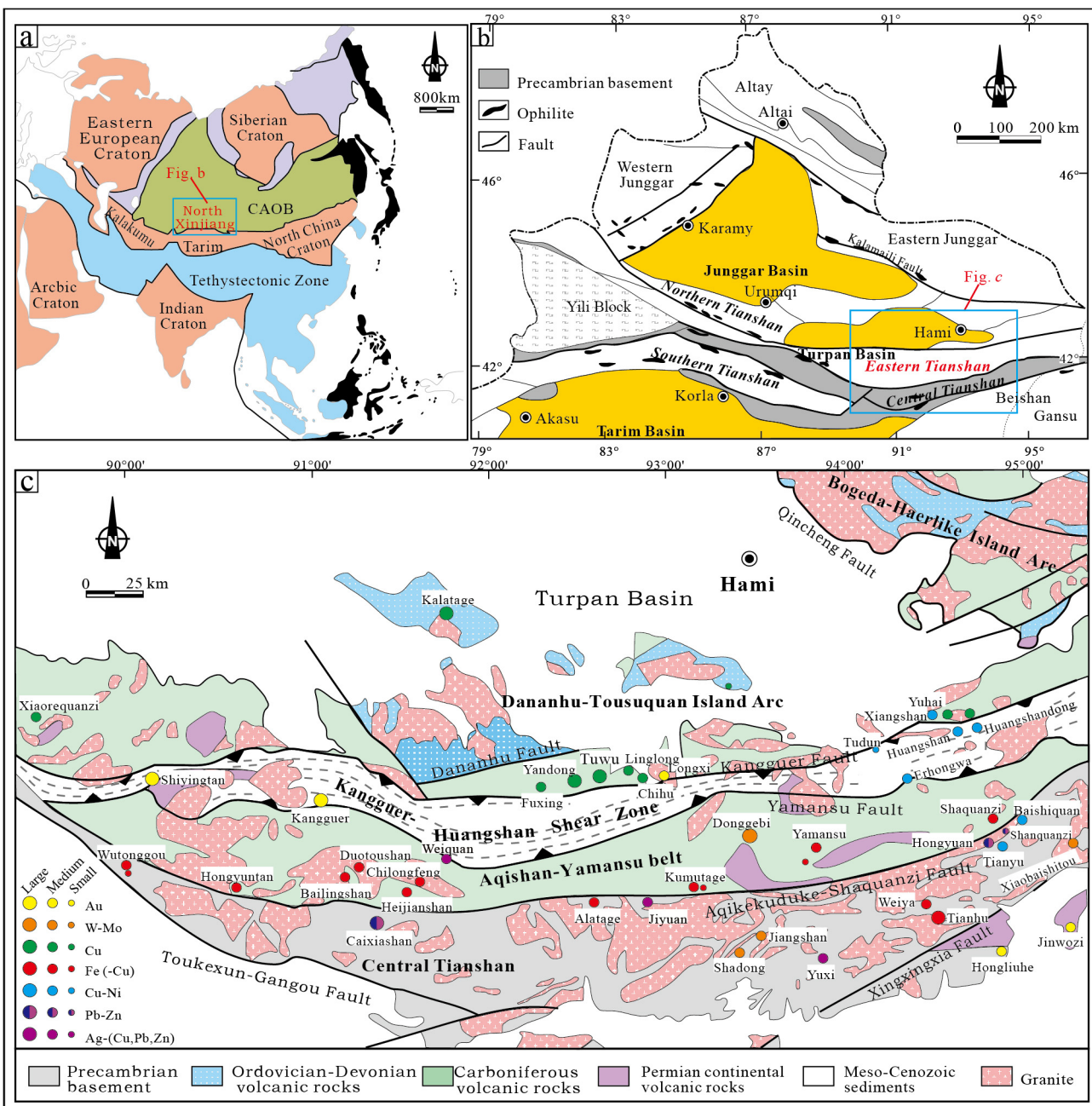


Fig. 1. (a) Location of northern Xinjiang in the Central Asia Orogenic Belt (modified after Huang et al., 2013a); (b) Sketch map showing the geological units of the Chinese Tianshan (modified after Pirajno et al., 2008); (c) Simplified geologic map of the Eastern Tianshan orogen (modified after Wang et al., 2006).

(Fig. 1c; e.g., Mao et al., 2005; Xiao et al., 2004). However, tectonic settings of the Carboniferous Aqishan-Yamansu belt have been variably attributed to: 1) backarc basin caused by the south-dipping subduction of the Junggar Ocean (Hou et al., 2014a); 2) island arc resulted from the north-dipping subduction of the South Tianshan Ocean (Xiao et al., 2004; Han et al., 2006); 3) island arc relate to a bipolar subduction of the Kangguer Ocean, generating the Aqishan-Yamansu belt in the south and the Dananhu-Tousuquan belt in the north (Wang et al., 2015; Du et al., 2018; Zhang et al., 2018).

The Aqishan-Yamansu belt hosts a total reserve of 207 Mt Fe @ 51% Fe and 20 kt Cu @ 0.06% Cu (Mao et al., 2005; Xu et al., 2011). Major deposits in the belt include the Shaquanzi, Duotoushan and Heijianshan Fe-Cu deposits, the Yamansu and Hongyuntan Fe (-Cu) deposits, and the Shuangfengshan, Heifengshan and Bailingshan Fe deposits (Fig. 1c; Table 1; Sang et al., 2003; Xu et al., 2011; Hou et al., 2014a; Jiang et al.,

2016; Zhao et al., 2016, 2017). Common features of these deposits include: 1) Carboniferous mineralization; 2) submarine volcanic/clastic rock-hosted; 3) magnetite as main ore mineral; 4) intensive and pervasive skarn alteration (e.g., garnet and pyroxene); 5) no clear spatial link with intrusions (Tables 1 and 2; Wu et al., 2006; Zhang et al., 2012a,b; Huang et al., 2013a; Huang et al., 2014; Hou et al., 2014a; Zhang et al., 2016a,b). The occurrence of skarn alteration with no apparent plutonic link has led to various hypotheses for the Fe-Cu metallogenesis: 1) skarn-type (e.g., Mao et al., 2005; Pirajno, 2013); 2) submarine volcanic-type, via interactions between magmatic-hydrothermal fluids and submarine rocks with seawater involvement (Hou et al., 2014a); 3) Iron-Oxide-Copper-Gold (IOCG) deposits (e.g., Huang et al., 2013a; Zhao et al., 2016, 2017). Besides, the Cu enrichment mechanism for some Cu-bearing deposits (such as Shaquanzi, Duotoushan and Heijianshan) has not been well-established (Table 1).

Table 1
Geological characteristics of the Fe (Cu) deposits in the Aqishan-Yamansu belt.

Deposit	Resource @grade	host-rocks	Occurrence	Alteration	Ore mineral	Gangue mineral	Data
Hongyuntan	Fe: M@?	Yamansu Fm.	Lenstoid, dipping 10° with the strata	Grt + Di + Act + Tr + Ep + Q + Ab + Mt + Kfs	Mt + Py + Cpy	Grt + Di + Act + Tr + Ep + Chl	Zhang et al. (2013), Zheng (2015)
Yamansu	Fe: 32 Mt@51%; Cu: 20000 t@ 0.06%		Stratiform, banded podiform to lenticular, orebodies mostly conformable with country rocks	Ep + Mt + Py	Mt + Py + Cpy + Hem	Grt + Hbl + Bt + Chl + Ep + Q + Cc	Mao et al. (2005), Hou et al. (2014a)
Shuangfengshan	Fe: ?@?	Tugutublak Fm.	Vein-type and lens-shaped hosted in the transitional zone between volcanic and sedimentary rocks	Grt + Ep + Chl + Py + Carb	Mt + Py	Grt + Ep + Chl + Cc + Q	Huang et al. (2013a,b)
Heifengshan	Fe: ?@?		Vein-type and lens-shaped	Grt + Ep + Chl + Py + Carb	Mt + Py	Grt + Ep + Chl + Cc + Q	Huang et al. (2013a,b)
Bailingshan	Fe: 13.06Mt@ 44.94	Fe: 2.49Mt@ 26–49%Cu: 2040 t@ 0.23–1.58%	Vein-type	Grt + Ep + Act	Mt + Py + Hem	Q + Ep + Act + Grt + Chl	Wang et al. (2005)
Shaquanzi		Fe: M@?Cu: sub-economic @?	Lenstoid to tabular	Grt + Ep + Kfs + Chl + Carb	Mt + Cpy + Py + Hem + Sph	Grt + Ep + Kfs + Q + Chl + Cc + Am + Di	Jiang et al. (2016)
Heijianshan	Fe: 12.06Mt@ 43.32%Cu: 0.38Mt@0.78%		Tabular or layered, almost parallel to the strata	Ep + Tur + Ser	Mt + Hem + Elt + Py + Po + Cpy	Ep + Cc + Am + Q + Chl	Zhao et al. (2017)
Duotoushan			Stratabound	Grt + Cpx + Amp + Ep + Chl + Ab	Mt + Cpy + Py	Grt + Cpx + Cam + Ab + Ep + Chl + Q + Cc	Zhang et al. (2017)

Abbreviations: M-Medium sized; ?-no published concrete data; Fn.-Formation; Alterations: Amp-ampibolite; Ab-albite; Act-actinolite; Carb-carbonate; Chl-chlorite; Di-diopside; Ep-epidote; Grt-garnet; Hem-hematite; Kfs-K-feldspar; Mt-magnetite; Mc-microcline; Preh-prehnite; Py-pyrite; Q-quartz; Scp-scapolite; Ser-sericite; Tur-tourmaline; Tr-tromolite;
Ore minerals: Au-gold; Bn-bornite; Cct-chalcopyrite; Cpy-chalcocite; Elt-electrum; Hem-hematite; Mt-magnetite; Po-pyrrhotite; Sph-sphalerite;
Gangue minerals: Ab-albite; Act-actinolite; Ah-Allanite; Anh-anhydrite; Ap-apatite; Bt-biotite; Cal-calcite; Cam-clinoamphibole; Chl-chlorite; Cpx-cliproxene; Di-diopside; Ep-epidote; Grt-garnet; Ilm-ilmenite; Kfs-K-feldspar; Mc-microcline; Or-orthoclase; Pmp-Pumpellyite; Preh-prehnite; Q-quartz; Ser-sericite; Sep-scapolite; Tun-Titanite; Tur-tourmaline.
 @? means the grade is not known.

Table 2

Isotopic ages of Fe (-Cu) deposits in the Aqishan-Yamansu belt.

Deposit	Dated mineral	Age (Ma)	Method	Data source
Shaquanzi	Magnetite	303 ± 12	Re-Os	Huang et al. (2014)
	Pyrite	294.5 ± 6.4	Re-Os	Huang et al. (2013b)
Shuangfengshan	Pyrite	292.4 ± 4.8	Re-Os	Huang et al. (2013b)
Heifengshan	Pyrite	301.5 ± 5.4	Re-Os	Huang et al. (2013b)
Yamansu	Zircon from skarn	323.47 ± 0.95	LA-ICP-MS U-Pb	Hou et al. (2014a)
	Zircon from diabase	335 ± 1.7	SHRIMP U-Pb	Li et al. (2014)
	Pyrite	322 ± 7	Re-Os	Huang et al. (2018)
	Zircon from synsite	335 ± 1.7	LA-ICP-MS	Wang et al. (2016)
Heijianshan	Zircon from basalt	306.2 ± 4.0	SHRIMP U-Pb	Zhang et al. (2012a,b)
Duotoushan	pyrite	312 ± 24	Re-Os	Zhang et al. (2017)
Bailingshan	Zircon	317.7–307.2	LA-ICP-MS	Zhang et al. (2016a,b)
Hongyuntan	Zircon from granitoids	328.5 ± 9.3	LA-ICP-MS U-Pb	Wu et al. (2006)
	zircon	324.1 ± 3.1		
	zircon	297.36 ± 0.51		Zheng (2015)

In this paper, we present a comprehensive review on the Aqishan-Yamansu Fe (-Cu) deposits, especially with regards to their ore deposit geology, age, alteration/mineralization paragenesis and ore fluid geochemistry, and discuss their ore deposit type and genesis under the regional geological context of the Aqishan-Yamansu belt.

2. Geological setting

The Chinese Tianshan lies in the southern part of the CAOB, and can be tectonically divided into the North-, Central-, and South Tianshan and the intervening Yili block (Fig. 1b) and geographically into the Eastern Tianshan and Western Tianshan along longitude 88°E (Xiao et al., 2004; Charvet et al., 2007; Li et al., 2008a,b; Gao et al., 2009; Han et al., 2011; Xiao et al., 2013).

The EW-trending Eastern Tianshan orogen comprises (from north to south) the Bogeda-Haerlike belt, Dananhu-Tousuquan magmatic arc, Kangguer-Huangshan ductile shear zone, Aqishan-Yamansu belt and the Central Tianshan, with the Qincheng, Kangguer, Yamansu and Aqikekuduke-Shaquanzi faults as their boundaries, respectively (Fig. 1c; Qin et al., 2002; Xiao et al., 2004; Mao et al., 2005; Su et al., 2011; Jiang et al., 2016).

The Bogeda-Haerlike belt mainly contains Ordovician-Carboniferous volcanics, granites and mafic-ultramafic complexes (Li, 2004); The Central Tianshan consists of a Precambrian crystalline basement (including the Tianhu, Xingxingxia and Kawabulake Groups), which comprises mainly meta-granites, granitic gneiss and biotite schist, which is unconformably covered by Paleozoic volcanic-sedimentary rocks intruded by numerous early Paleozoic to early Mesozoic ultramafic to felsic rocks (Xiao et al., 2004; Su et al., 2013). Some metamorphosed sedimentary Fe deposits (e.g., Tianhu and Yushan) and some sediment-hosted Pb-Zn (-Ag) deposits (Caixiasan, Hongyuan and Yuxi) were discovered in the Central Tianshan (Wang et al., 2006).

The Dananhu-Tousuquan magmatic arc contains mainly the Qi'eshan Group (ca. 336–320 Ma) basaltic to andesitic volcanics, locally overlying the Lower Carboniferous carbonates and calcareous mudstone and overlain by the Upper Carboniferous Tuwu Formation grey-wacke, tuff and carbonate interbeds (Hou et al., 2005; Li et al., 2005; Mao et al., 2005). Volcanics of the Permian Aqikebulak Formation include basalt, tuff, and volcanic breccia. Local outcrops of the Jurassic Xishanyao Formation terrestrial siliciclastics are also present (Mao et al., 2005). Porphyry Cu deposits (e.g., Tuwu-Yandong) and VMS deposit (e.g., Kalatage) were hosted in this belt (Hou et al., 2005; Wang et al., 2006).

The Kangguer-Huangshan ductile shear zone contains mainly Carboniferous mylonite, tectonic lenses, breccias and fine sandstone and carbonaceous siltstone with local bimodal volcanic interbeds (Chen et al., 2003; Huang et al., 2014; Mao et al., 2005). The sedimentary-volcanic sequences were low-grade metamorphosed and exhibit

cleavages (Su et al., 2011). Mylonite, tectonic lenses and breccias are distributed along early extensional faults (Qin et al., 2002; Xu et al., 2003). Ductile shear zone-hosted Au deposits (e.g., Shiyingtan and Kangguer) are hosted in this belt (Wang et al., 2006).

The Aqishan-Yamansu belt, is bounded by the Yamansu fault and Aqikekuduke fault in the north and south, respectively. Lithostratigraphy includes mainly the Lower Carboniferous Yamansu Formation in the northern part, the Upper Carboniferous Tugutublak Formation in the southern part and the local Permian Aqikebulak Formation (Muhettaer et al., 2015; Zhang et al., 2016a,b; Fig. 2). The Yamansu Formation can be subdivided into three members: The lower member contains mainly greenish-gray mafic to intermediate tuff, volcanic breccia, and medium to fine sandstone with minor bioclastic limestone intercalation. The middle member consists of felsic tuff, coarse sandstone, and mixtite, intercalated with bioclastic or micro-crystalline limestone. The upper member contains limestone and minor tuff and sandstone (Fig. 2; Qin et al., 2002; Zhang et al., 2012a,b).

The Tugutublak Formation (aka. Dikaner/Matoutan/Shaquanzi Formation) unconformably overlies the Yamansu Formation and comprises a flysch assemblage (Mao et al., 2005; Zuo et al., 2006; Zhang et al., 2012a,b; Xu et al., 2014). The Tugutublak Formation also contains three members: The lower member consists of aubergine andesite, rhyolite flows, crystal tuff and tuffaceous lava, and intercalated with volcanic breccia, agglomerate, limestone and sandstone; The middle member contains volcanic breccia, tuff, sandstone and limestone; The upper member is dominated by purplish-gray andesite and gray basaltic lava with minor purple-colored rhyolite and sandstone interbeds. Marine fossils, such as corals and fusulinids, were identified in some layers of these three formations (Fig. 2; Zhang et al., 2012a,b).

The Permian Aqikebulak Formation unconformably overlies the Tugutublak Formation, and contains three members comprising mainly continental calc-alkaline to alkaline intermediate-felsic lava and pyroclastic rocks (Fig. 2; Liu, 2009).

The lower Paleozoic sequences were intruded by the Late Carboniferous to early-Middle Permian granitoids (Fig. 1c; Mao et al., 2005; Zhou et al., 2010; Lei et al., 2013).

In the Aqishan-Yamansu belt, many submarine volcanic-hosted Fe (e.g., Hongyuantan, Bailingshan) and Fe-Cu deposits (e.g., Heijianshan, Duotoushan and Shaquanzi) deposits have been discovered (Wang et al., 2006; Han et al., 2014; Hou et al., 2014b). These deposits are mainly hosted in the Carboniferous submarine volcanic/clastic rocks of the Yamansu and Tugutublak formations, with the Cu-rich ones being hosted predominantly in the latter (Wang et al., 2006; Han et al., 2014; Hou et al., 2014b; Jiang et al., 2016; Zhang et al., 2016a,b; Zhao et al., 2016, 2017).

The tectonic framework of the Eastern Tianshan was grossly related to the evolution of two ocean basins, i.e. 1) the Junggar Ocean between the Central Tianshan and Junggar terranes; and 2) the South Tianshan

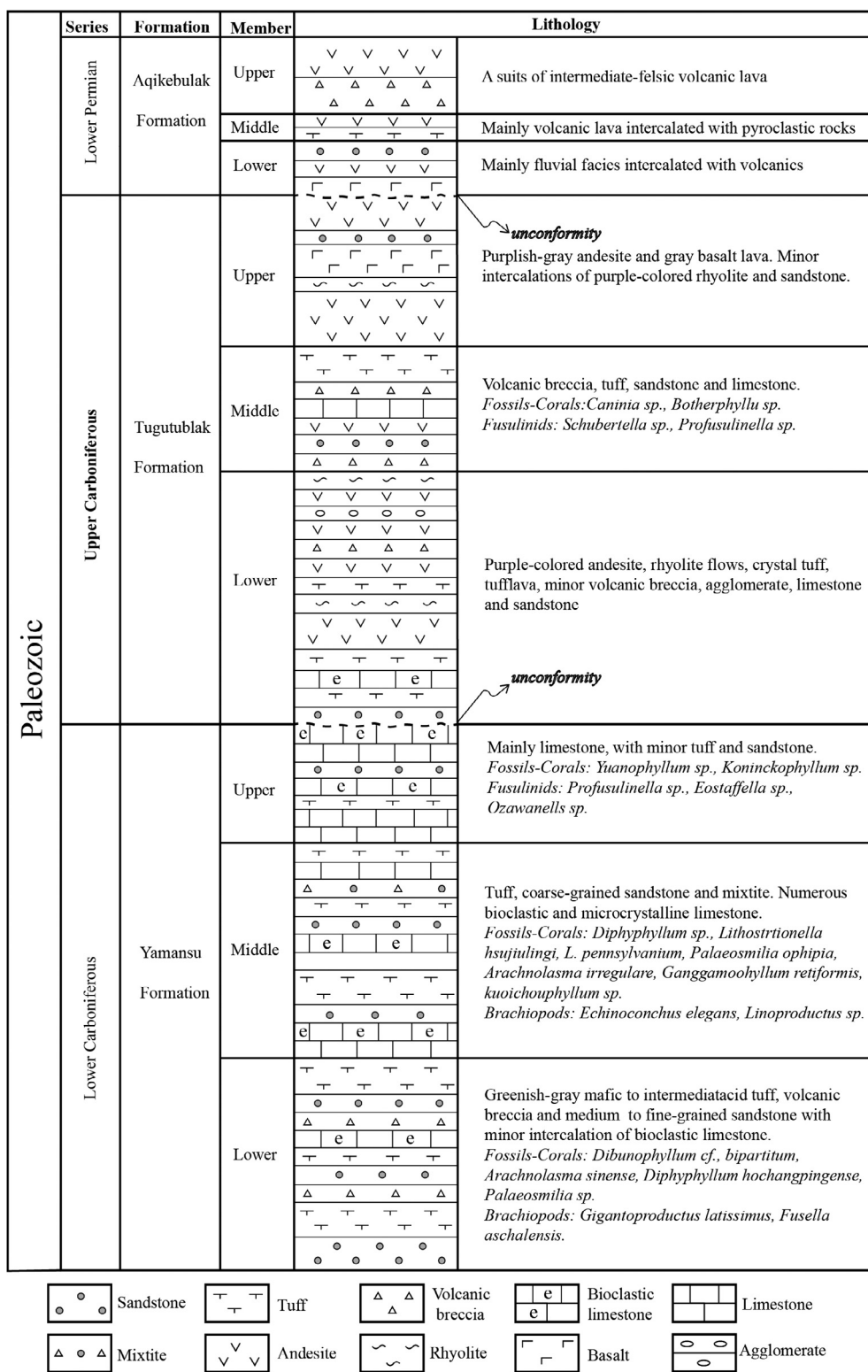


Fig. 2. Composite stratigraphic column of the Paleozoic Aqishan-Yamansu belt (compiled after Zuo et al., 2006; Luo et al., 2012; Zhang et al., 2012a,b, 2016a,b).

Ocean between the Central Tianshan and Tarim terranes (e.g., Xiao et al., 2004).

3. Carboniferous magmatism in the Aqishan-Yamansu belt

Lithology in the Aqishan-Yamansu belt consist mainly of volcanic rocks including the Yamansu and Tugutublak formations and

intermediate-felsic intrusions with various ages. Studies and summarizing on geochronology and geochemistry of the volcanics and intrusions will help us to define the Carboniferous tectonic setting of this significant mineralization belt.

3.1. Geochronology of volcanic rocks and intrusions

3.1.1. Volcanic rocks

Volcanic rocks in the Aqishan-Yamansu belt mainly consists of the Lower Carboniferous Yamansu Formation in the northern part and the Upper Carboniferous Tugutublak Formation in the southern part (e.g., Muhetaer et al., 2015; Zhang et al., 2016a,b; Fig. 2).

As for the Yamansu Formation, Luo et al. (2012) reported LA-ICP-MS zircon U-Pb ages for dacites from the eastern (ca. 348 Ma), central (ca. 336 Ma) and western (ca. 334 Ma) parts of the belt. LA-ICP-MS zircon U-Pb age of 336 Ma was obtained for the basaltic andesite (Luo et al., 2015). Hou et al. (2014a) obtained an age of ca. 324 Ma based on seven zircons selected from the basalts. These results suggest that the Yamansu Formation volcanic rocks were emplaced during the Early Carboniferous (ca. 348 – 324 Ma).

As for the Tugutublak Formation, LA-ICP-MS zircon U-Pb ages were reported for the rhyolites (320 Ma; Li et al., 2011), basaltic andesite (321 Ma and 319 Ma; Luo et al., 2015) and tuffaceous dacitic lava (at Bailingshan: 324.1 Ma; Zhang et al., 2016a,b). Combined with the ages of andesite (314.7 Ma) and andesitic tuff (305.3 Ma) in the Shazuanzi area (Jiang et al., 2017), the emplacement age of the Tugutublak Formation volcanics is constrained to be around 324–305 Ma.

At the same time, inherited zircons with ages of 545 Ma, 488 Ma, 440 Ma, 370 Ma, 700–1000 Ma, 1400 Ma, 2200 Ma, 2600 Ma, peaking at ca. 600, 1000, 1400, 2200 and 2600 Ma have also been identified in the Yamansu and Tugutublak Formation (Luo et al., 2015). These Precambrian ages indicate the link between the volcanics and the Central Tianshan.

3.1.2. Intrusions

Early Carboniferous to Triassic intermediate-felsic intrusions intruded the Yamansu and Tugutublak Formations (Supplementary Table 1). Early Carboniferous plutons include the Xifengshan (349 Ma) and Shiyingtan (342 Ma) granites and the Changtiaoshan quartz diorite (337 Ma) (Zhou et al., 2010). At the Hongyuntan Fe deposit, Carboniferous quartz monzonodiorite (351.5 Ma) and biotite monzogranite (326.8 Ma) have been identified (Zheng, 2015). Recently, Du et al. (2018) reported Early Carboniferous age for the granodioritic pluton (336 Ma) near the Aqishan Mountain.

Late Carboniferous intermediate-felsic plutons include the granite porphyry (316.3 Ma) and monzonitic granite (318.3 Ma) at the Duotoushan Fe-Cu deposit (Zhang et al., 2017), the biotite diorite (316.7 Ma), and granodiorite (305.8 Ma) in the Heijianshan-Chilongfeng area (Zhao et al., 2018), as well as the Bailingshan granodiorite (317.7 Ma), monzonitic granite (313.7 Ma) and granite (307.2 Ma) in the Bailingshan area (Zhang et al., 2016a,b).

3.2. Geochemical characteristics

3.2.1. Volcanic rocks

The emplacement of the Yamansu and Tugutublak formations occurred during ca. 350–325 Ma and 325–300 Ma, respectively. From the few published geochemical studies on the two formations (Supplementary Table 2; e.g., Luo et al., 2015; Wang et al., 2016), the volcanics were suggested to have originated from subduction-related settings without significant crustal contamination (Fig. 3a). The variable Ba/La and relatively uniform Th/Yb of the Yamansu and Tugutublak Formation indicate that their mantle source may be metasomatized by slab-derived fluids (Fig. 3b). As displayed in Fig. 3c, the Yamansu and Tugutublak basalts show mixed compositions of MORB and VAB. Rocks with such compositions commonly formed in fore-arc basin (Reagan et al., 2010; Morishita et al., 2011) or back-arc basin (Fan et al., 2010; Shuto et al., 2006).

To sum up, the emplacement of the Yamansu and Tugutublak Formation should be resulted from the subduction mechanism (forearc basin or backarc basin) with the mantle source enriched by slab-derived

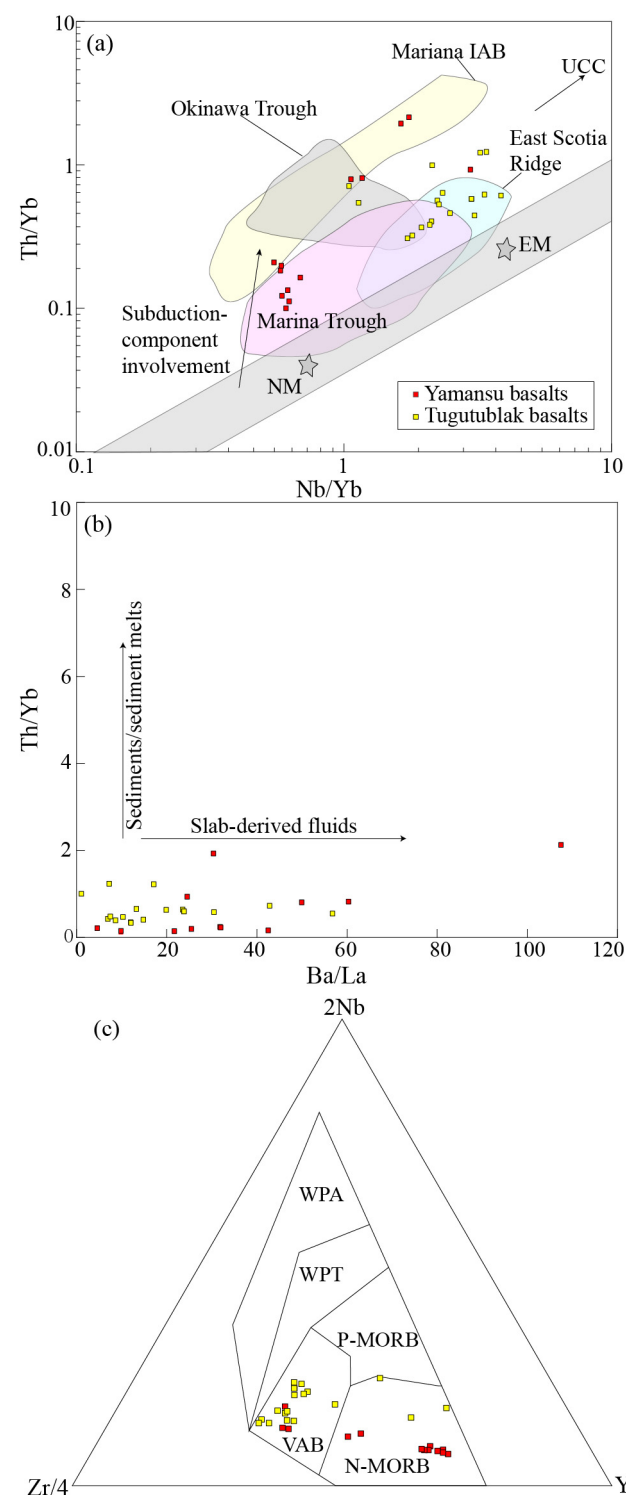


Fig. 3. Tectonic discrimination diagrams of the Carboniferous basaltic rocks in the Aqishan-Yamansu belt (a) Th/Yb vs. Nb/Yb (after Pearce, 2008); (b) Th/Yb vs. Ba/La (after Woodhead et al., 2001); (c) 2Nb-Zr/4-Y ternary diagram (after Meschede, 1986). Abbreviations: NM- N-MORB; EM- E-MORB; IAB- island arc basalt; CAB- continental arc basalt; WPT- within-plate tholeiites; WPA- within-plate alkaline basalt; VAB- volcanic arc basalt.

fluids.

3.2.2. Intrusions

Early and late Carboniferous intermediate to felsic intrusions in the belt include the those in the Hongyuntan and Duotoushan Fe (-Cu)

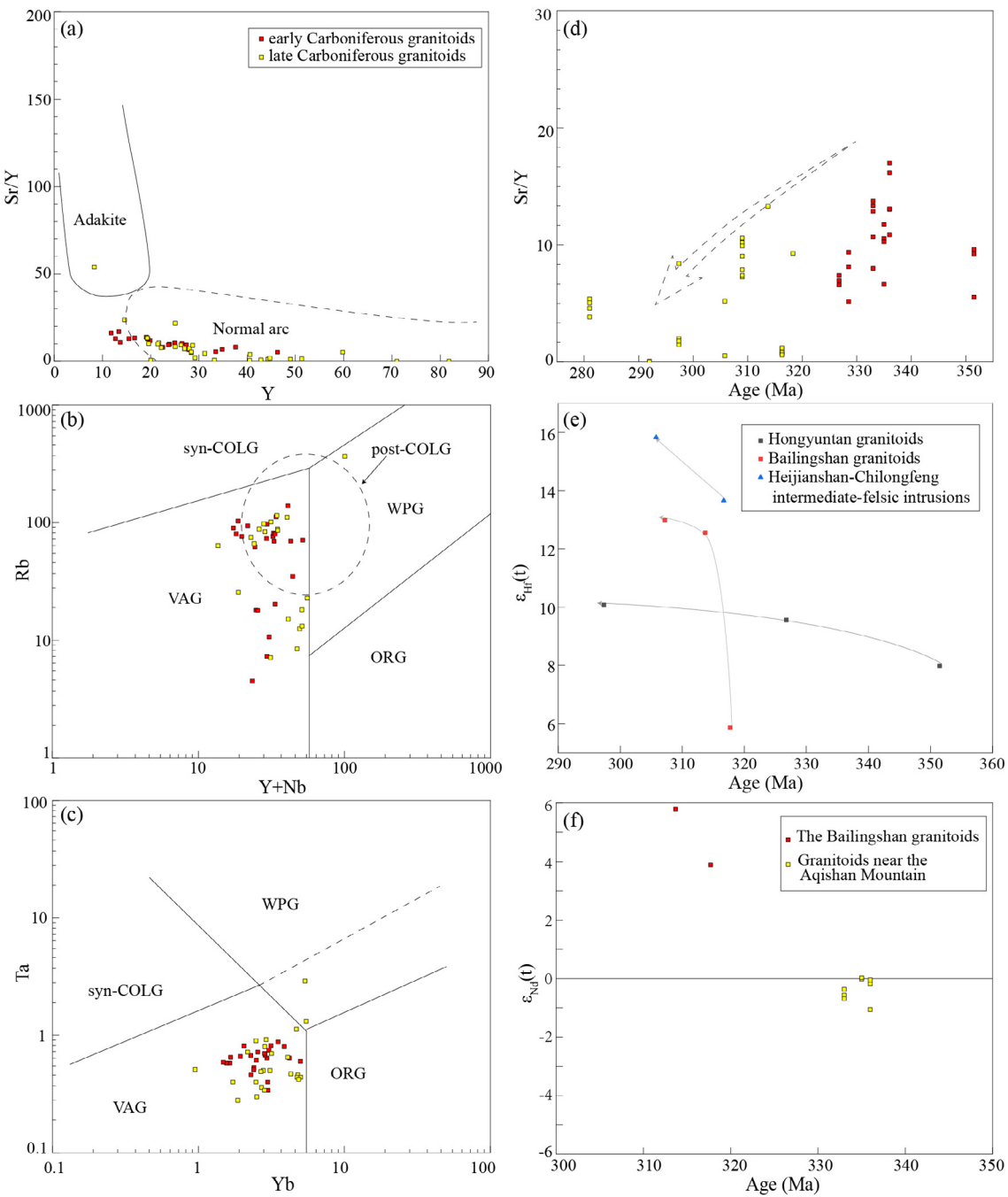


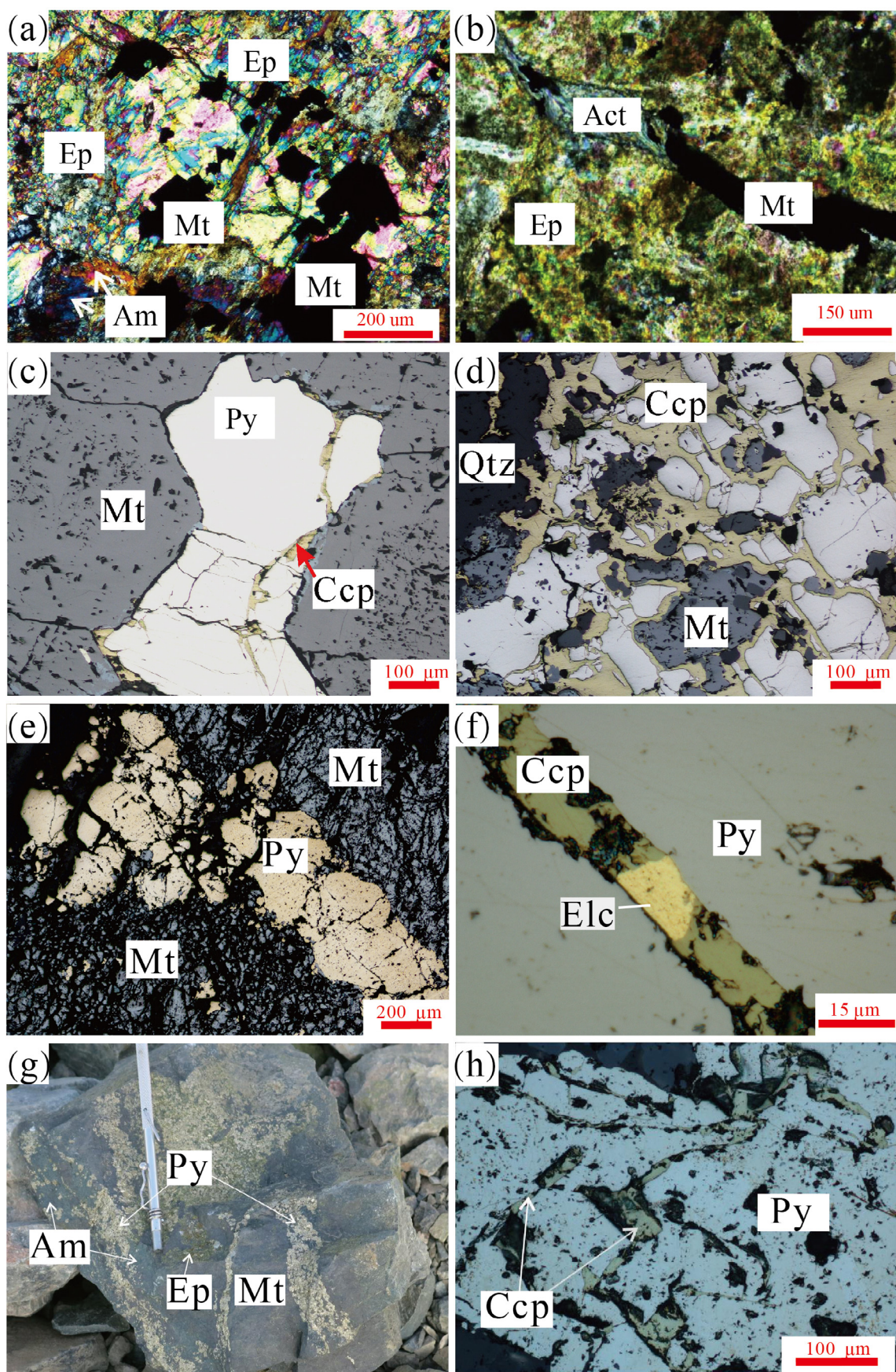
Fig. 4. Tectonic discrimination diagrams of the Carboniferous Aqishan-Yamansu granitoids (a) Sr/Y vs. Y diagram (after Defant and Drummond, 1990); (b) Rb vs. $(\text{Y} + \text{Nb})$ diagram (after Pearce, 1996); (c) Ta vs. Yb diagram (after Pearce et al., 1984). (d) Sr/Y vs. zircon U-Pb age diagram; (e) Average zircon $\epsilon_{\text{Hf}}(\text{t})$ vs. zircon U-Pb age; (f) Whole rock $\epsilon_{\text{Nd}}(\text{t})$ vs. zircon U-Pb age. Abbreviations: VAG- volcanic arc granite; syn- COLG-syn-collision granite; WPG- within-plate granite; ORG- ocean ridge granite.

deposits, the Bailingshan granitoids, the intermediate-felsic intrusions in the Heijianshan-Chilongfeng area and those near the Aqishan Mountain (Supplementary Table 2). Based on the compiled data, all the Carboniferous granitoids show relatively low Sr/Y values, which are distinguished from adakites but comparable to normal arc magmas (Fig. 4a), indicating that these granitoids should be arc-related, which could be further supported by the Rb vs. $\text{Y} + \text{Nb}$ and Ta vs. Yb diagram (Fig. 4b, c). Meanwhile, the Sr/Y display an overall decreasing trend from the Early to Late Carboniferous (Fig. 4d). The Bailingshan granitoids show positive zircon $\epsilon_{\text{Hf}}(\text{t})$ values and whole rock $\epsilon_{\text{Nd}}(\text{t})$ values, and the zircon $\epsilon_{\text{Hf}}(\text{t})$ values gradually increased with time (Fig. 4e). This kind of trend can also be observed in the Hongyutan granitoids

and the Heijianshan-Chilongfeng intermediate-felsic intrusions, respectively (Fig. 4e), indicating the increasing contributions of mantle materials, which is consistent with Du et al. (2018). Early Carboniferous granitoids near the Aqishan Mountain have $\epsilon_{\text{Nd}}(\text{t})$ values ranging between -1.06 and 0.03 , but the late Carboniferous Bailingshan granitoids have $\epsilon_{\text{Nd}}(\text{t})$ values ranging between 3.89 and 5.78 (Fig. 4f; Supplementary Table 3).

4. Ore deposit geology

Ore deposits in the Aqishan-Yamansu belt could be divided into Fe-only and Fe-Cu ones (Table 2).



(caption on next page)

Fig. 5. (a) Magnetite coexists with epidote and minor amphibole (Duotoushan); (b) Magnetite coexists with actinolite and cut epidote (Heijianshan); (c) Smooth contact between magnetite and pyrite (Shaquanzi), indicating intergrowth relationship; (d) Magnetite, pyrite and quartz replaced by chalcopyrite (Shaquanzi); (e) Pyrite vein crosscuts massive magnetite (Heijianshan); (f) Massive pyrite crosscut by chalcopyrite and electrum vein (Heijianshan); (g) Massive magnetite (intergrown with minor amphibole and epidote) crosscut by pyrite veins (Duotoushan); (h) Chalcopyrite veins crosscut pyrite veins (Duotoushan). Jiang, Zhang, and Zhao provided the figures.

4.1. Mineralization age

As for the Fe-only deposits, Hou et al. (2014a) obtained a mean weighted age of 323.47 ± 0.95 Ma for the magmatic zircons in the skarn of the Yamansu Fe deposit. Diabase dikes (335 ± 1.7 Ma) and syenite (325.5 ± 1.7 Ma) crosscutting the skarn and Fe orebodies at Yamansu provided a lower limit for the mineralization age (zircon U-Pb; Li et al., 2014; Wang et al., 2016). A Re-Os isochron age of 322 ± 7 Ma for the pyrite associated with magnetite has recently been reported (Huang et al., 2018). All these data suggest that the Yamansu Fe mineralization during ca. 335–320 Ma.

Zhang et al. (2016a,b) concluded that the Bailingshan Fe mineralization occurred during 317.7–307.2 Ma based on zircon U-Pb data of the granitoids there and crosscutting relationships. Similarly, Zheng (2015) concluded the Hongyuntan Fe deposit was formed during 328–300 Ma according to the ages of quartz keratophyre (324.1 ± 3.1 Ma) and moyite (297.36 ± 0.51 Ma). The Heifengshan and Shuangshan Fe deposits yielded pyrite Re-Os isochron ages of 310 ± 23 Ma and 292 ± 5 Ma, respectively (Huang et al., 2013b).

For the Fe-Cu deposits, Re-Os isochron dating of magnetite and the coexisting pyrite from Shaquanzi yielded 303 ± 12 Ma and 295 ± 7 Ma (Huang et al., 2014). At Duotoushan, the sulfide mineralization was estimated to be 312 ± 24 Ma (pyrite Re-Os isochron age; Zhang et al., 2017). At Heijianshan, Zhang et al. (2012a,b) suggested the basalt as the source for the *syn*-volcanic Cu mineralization and adopted the SHRIMP U-Pb age of the basalt (306.2 ± 4.0 Ma) to be the mineralization age.

Taken together, the Fe (-Cu) mineralization in the Aqishan-Yamansu belt could be divided into two types: The early Carboniferous Fe deposits (Yamansu deposit: 335–325.5 Ma; Hongyuntan Fe deposit: mineralization from ca. 328 Ma), the Late Carboniferous Fe (-Cu) deposits formed during ca. 320–300 Ma.

4.2. Host rocks

In the Aqishan-Yamansu belt, the Yamansu Formation hosts the Yamansu (Hou et al., 2014a), and Hongyuntan Fe deposits (Zhang et al., 2013), whilst the Tugutubulak Formation hosts the Shaquanzi (Jiang et al., 2016, 2017), Heijianshan (Zhao et al., 2016, 2017) and Duotoushan Fe-Cu deposits (Zhang et al., 2017) and the Shuangfengshan, Heifengshan (Huang et al., 2013a) and Bailingshan Fe deposits (Wang et al., 2005; Zhang et al., 2016a,b) (Fig. 2; Table 1).

Most of the Aqishan-Yamansu Fe (-Cu) orebodies are vein-type and lensoidal (Table 1). Some orebodies occur in the transitional zone between volcanic and sedimentary rocks, e.g., the Yamansu deposit (Huang et al., 2013a; Hou et al., 2014a).

Table 3

Temperatures and salinities for the ore-forming fluids of the Fe (-Cu) deposits in the Aqishan-Yamansu belt.

Deposit	stage	hosted mineral	FI type	measured FI	Te(°C)	Tm(°C)	Th (°C)	Salinity (wt%)	Data source
Shaquanzi	Magnetite	Quartz	PC, S,W	W	–55.1–49.0 –66.4–43.9	–18.0–13.4 –25.9–1.0	573–348 314–103	20.9–22.3 17.7–24.6	Jiang et al. (2016)
	Chalcopyrite	Calcite			–70.8–38.1	–58.1	536–301	W:21.2–22.78 S:16.4–56.0	Zhao et al. (2017)
Heijianshan	Magnetite	Quartz	W, S	W, S		–81.3–51.3	–52.4–15.8	262–119	W:19.0–23.1 S: 34.5–34.7
	Cu-Au								
Hongyuntan Yamansu	Magnetite	Epidote	W	W		–12–1	150–397 330–340	0.18–15.96 2.7–12.9	Zheng (2015) Mao et al. (2005)
	Magnetite								

4.3. Alteration/mineralization paragenesis

The Fe (-Cu) deposits in the Aqishan-Yamansu belt could be divided into the Early Carboniferous Fe deposits (Yamansu and Hongyuntan), Late Carboniferous Fe-Cu deposit (Shaquanzi, Duotoushan, Heijianshan) and the Late Carboniferous Fe deposit (Shuangfengshan, Heifengshan, Bailingshan).

As for the Early and Late Carboniferous Fe deposits, e.g., Yamansu and Bailingshan, respectively, the alteration/mineralization comprises the prograde skarn, retrograde alteration, sulfide mineralization (with a few chalcopyrite) and supergene alteration stages, with garnet forming in the prograde stage and magnetite in the retrograde stage along with epidote, chlorite and amphibole. The orebodies of the Early Carboniferous Fe deposits are commonly stratabound within the volcanic lava and clastic sequences, suggesting *syn*-volcanic/sedimentary mineralization. This is supported by the similar ages between the skarn (ca. 323.5 Ma) and volcanic rocks (ca. 324.4 Ma) (Hou et al., 2014a).

As for the Late Carboniferous Fe-Cu deposits, it shares similar alteration features with the Carboniferous Fe deposits with respect to the development of both prograde skarn and retrograde alteration, and the coexistence of magnetite mineralization with the latter (Fig. 5a). The Heijianshan deposit is exceptional in terms of the absence of skarn alteration and the development of epidote alteration before magnetite mineralization (Fig. 5b). Meanwhile, some electrum could also be observed at Heijianshan (Fig. 5f).

It is noteworthy that Fe mineralization commonly preceded Cu mineralization in the Aqishan-Yamansu Fe-Cu deposits (Jiang et al., 2016; Zhang et al., 2016a,b; Zhao et al., 2016, 2017). At Shanquanzi, the smooth magnetite-pyrite grain contact indicates their coeval formation (Fig. 5c), whilst the replacement of magnetite, pyrite and quartz by chalcopyrite indicates that the Cu mineralization was formed later (Fig. 5d). The massive magnetite at Heijianshan was crosscut by pyrite veins (Fig. 5e) and then by chalcopyrite and electrum veins (Fig. 5f), also suggesting a later Cu (-Au) mineralization. Similarly, the massive magnetite (intergrown with minor amphibole and epidote) at Duotoushan was crosscut by pyrite veins and then by chalcopyrite veins, indicating the consecutive formation of magnetite, pyrite and then chalcopyrite (Fig. 5g, h).

To summarize, hypogene alteration/mineralization in the Aqishan-Yamansu Fe deposits commonly comprise an early Ca-Na-K alteration, the main magnetite mineralization and a late ore-barren veining stage (dominating by quartz and carbonate). For the Fe (-Cu) deposits, the Cu mineralization always occurred after the Fe mineralization.

4.4. Nature of the ore-forming fluids

Published fluid inclusion (FI) types and their ice-melting

temperatures, homogenization temperatures and salinities from the major Aqishan-Yamansu Fe (-Cu) deposits are summarized in Table 3. These FIs are mostly W-type (aqueous), S-type (solid-bearing) and C-type (carbonic-aqueous) (Jiang et al., 2016; Zhao et al., 2017). For the sake of clear discussion, we only focused on the main mineralization stages.

As for the Yamansu Fe deposit, the Fe ore-forming fluid temperatures are of 340–330 °C, with salinities of 12.9–2.7 wt% NaCl equiv. (Mao et al., 2005). As for the Hongyuntan Fe deposit, FIs in the epidote coexisting with magnetite homogenized at 150–397 °C (peak at 300 °C) and have salinities of 0.18–15.96 wt% NaCl equiv. (Zheng, 2015).

The Aqishan-Yamansu Fe-Cu deposits contain wide ranges of homogenization temperatures and salinities (Table 3), indicating multiple ore fluid sources. At Shaquanzi, FIs from the Fe mineralization stage homogenized at 573–348 °C, consistent with the magnetite and quartz oxygen isotope thermometric calculations (570–470 °C) (Jiang et al., 2016). Fluid inclusions from the Cu mineralization stage homogenized at 314–103 °C (peak at 160 °C) (Jiang et al., 2016). The marked homogenization temperature drop from the Fe- to Cu mineralization stage suggests cooling, possibly with low-temperature fluid incursion. Based on the eutectic and ice melting temperatures, a Ca-rich ore-

forming fluid was deduced (Fig. 6a–f; Davis et al., 1990; Chen et al., 2011). Salinities of Ca-rich fluids were calculated according to the method of Chi and Ni (2007), which yielded 20.9–22.3 wt% NaCl eq. and 17.7–24.6 wt% NaCl eq. for the Fe- and Cu mineralization stage, respectively. Similar ore-forming fluid physicochemical properties and evolution were also identified at Heijianshan (Fig. 6g–l; Zhao et al., 2017). In general, the Fe and Cu mineralization fluids have similar features, such as high salinities and being Ca-rich, yet they differ in the higher homogenization temperatures in the former (usually > 300 °C).

4.5. Sources of metals and ore-forming fluids

Compilation of $\delta^{34}\text{S}$ values from the Aqishan-Yamansu Fe (-Cu) deposits is illustrated in Fig. 7. Magmatic signatures ($0 \pm 5\%$, Ohmoto and Rye, 1979; Hoefs, 1997) is distinct in the Fe mineralization stage in all of the deposits. In the Cu mineralization stage at Duotoushan and Shaquanzi, the ore-forming fluids have $\delta^{34}\text{S}$ values of 8.8–12.1‰ and $\geq 24.8\%$, respectively (Jiang et al., 2016; Zhang et al., 2017). The elevated $\delta^{34}\text{S}$ values may suggest the involvement of evaporite-sourced fluids and/or Carboniferous seawater or basinal brine (Fig. 7a, b; Thode, 1991; Chang et al., 2008; Jiang et al., 2016; Zhang et al., 2017;

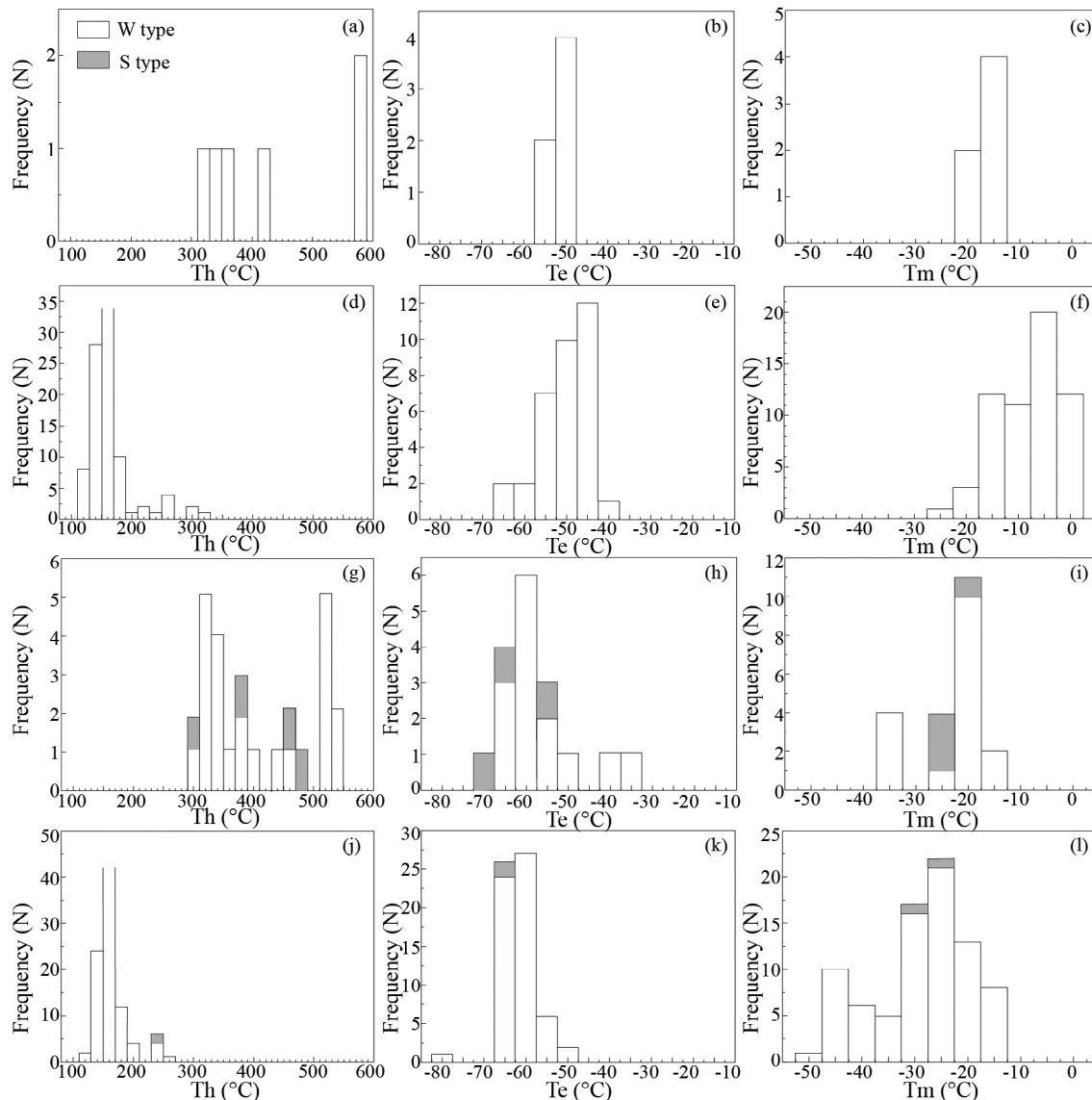


Fig. 6. Fluid inclusion homogenization temperature (Th), eutectic temperature (Te) and salinities for the Aqishan-Yamansu Fe (-Cu) deposits. A–c: Fe mineralization stage (Shaquanzi); d–f: Cu mineralization stage (Shaquanzi); g–i: Fe mineralization stage (Heijianshan); j–l: Pyrite stage (Heijianshan).

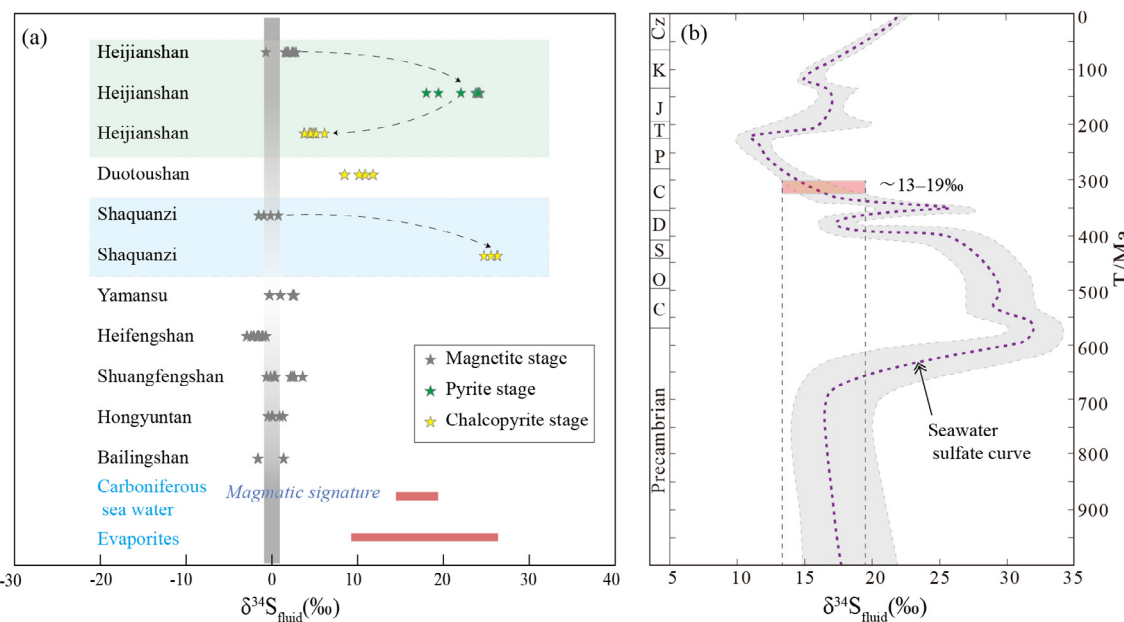


Fig. 7. (a) Sulfur isotopes of the Aqishan-Yamansu Fe (-Cu) deposits; (b) Sulfur isotopes of global seawater through geological time (after Chang et al., 2008).

Zhao et al., 2017). At Heijianshan, the calculated $\delta^{34}\text{S}$ values for the ore fluids are 1.7–4.3‰ (magnetite stage), 24.3–29.3‰ (pyrite stage), and 1.5–4.1‰ (Cu sulfide stage) (Zhao et al., 2017), which most probably show a gradual increase of the interaction with basinal brines and the andesite ore host. The elevated $\delta^{34}\text{S}$ values in the pyrite stage may suggest the involvement of evaporite-sourced fluids and/or Carboniferous seawater or basinal brine (Fig. 7a; Thode, 1991; Chang et al., 2008; Jiang et al., 2016; Zhang et al., 2017; Zhao et al., 2017). The magmatic-hydrothermal sulfur isotopic features and the low temperature fluids (< 300 °C), as well as the high salinities in the Cu ore fluids suggest that the sulfur and Cu for the Cu mineralization may have been leached from the andesite ore host, caused by the very intense water-rock interactions.

Based on these data, we propose that the Aqishan-Yamansu Fe ore fluids were largely magmatic, whilst the Cu mineralization was caused by Carboniferous seawater/basinal brine incursion.

5. Discussion

5.1. Tectonic evolution of the Aqishan-Yamansu belt

5.1.1. Relationship with the Precambrian Central Tianshan

Detrail zircons with older ages (370 Ma, 440 Ma, 488 Ma, 545 Ma, 700–1000 Ma, 1400 Ma, 2200 Ma, 2600 Ma) have been identified in the Yamansu (ca. 348–334 Ma) and Tugutubulak (ca. 325 Ma till the latest Carboniferous) formations of the Aqishan-Yamansu belt (e.g. Luo et al., 2012, 2015; Jiang et al., 2017).

In the Eastern Tianshan, Precambrian materials are only reported in the Central Tianshan based on its Precambrian basement which was divided into the Tianhu, Kawabulake and Xingxingxia Groups (Hu et al., 1998; Liu et al., 2004). Detrial zircons from sandstones, low-grade metamorphic schists, in the Central Tianshan give several Precambrian age populations (ca. 2.5–2.4 Ga, 1.9–1.8 Ga, 1.6–1.5 Ga, 1.0–0.9 Ga and 0.82–0.75 Ga; Ma et al., 2012a,b).

These indicate that the extremely old ages in the Aqishan-Yamansu belt were most likely inherited from the Central Tianshan. In other words, the Central Tianshan may provide a material source for the Aqishan-Yamansu belt during the Carboniferous and the earliest Permian period. Zhang et al. (2016a,b) even proposed that the Central Tianshan may be a topographic highland in the Carboniferous based on studies on detrial zircons in the sandstones in the Shaquanzi and

Yamansu area adjacent to the northern margin of the Central Tianshan.

5.1.2. Early Carboniferous formation of the Aqishan-Yamansu fore-arc basin

The closure of the South Tianshan Ocean between the eastern and western part is suggested to be diachronous, or a ‘scissors-like’ closure (Chen et al., 1999; Dong et al., 2011; Zong et al., 2012; He et al., 2014). In the western part, the final amalgamation may have completed in the Late Carboniferous with the collision between the Tarim and Central Tianshan-Yili blocks, based on garnet-growth ages (313–315 Ma) in the HP-UHP rocks (Klemm et al., 2011). In the eastern part, however, He et al. (2014) report a metamorphic overprint at ca. 380 Ma to the orthogneiss of the Xingxingxia Complex on the southern part of the Central Tianshan massif, pointing to a Devonian closure in the eastern part of the South Tianshan Ocean. Then, the formation of the Carboniferous Aqishan-Yamansu belt, located in the Eastern Tianshan, was unlikely to be related to the north-dipping subduction of the South Tianshan Ocean. This is supported by the lacking of subduction-related igneous activities younger than ca. 380 Ma in the southern part of the Central Tianshan massif (Zhang et al., 2015).

The Kangguertage ophiolite (SHRIMP zircon U-Pb age: 494 ± 10 Ma, Li et al., 2008a,b) in the Dananhu-Tousuquan belt points to a late Cambrian opening of the Junggar Ocean. Pelagic fossils (e.g., corals and brachiopods) in the Yamansu Formation and the Middle Member of the Tugutubulak Formation (Fig. 2; Chen et al., 2003; Su et al., 2009; Zhang et al., 2012a,b) suggest the existence of ocean basin until at least the Late Carboniferous.

Recent studies on arc-featured granitoids in the Dananhu-Tousuquan arc reveal the north-dipping subduction of the Kangguer Ocean started no later than ca. 380 Ma (Fig. 8; Xiao et al., 2017), which is also supported by the Devonian granitoids in the Kangguer shear zone and the Dananhu-Tousuquan arc (Fig. 8). In contrary, the general distribution of the Early to Late Carboniferous arc-featured granitoids and volcanic rocks in the Aqishan-Yamansu belt suggest that the south-dipping subduction of the Kangguer Ocean started at ca. 350 Ma (Figs. 3, 4, 8; Supplementary Table 4).

As stated above, the Carboniferous granitoids in the Aqishan-Yamansu belt all show arc geochemical features (Fig. 4a, b). Meanwhile, the Early Carboniferous Yamansu Formation and Late Carboniferous Tugutubulak Formation displayed MORB-VAB mixed affinity, which were most likely formed in a forearc or backarc basin (Fig. 3c).

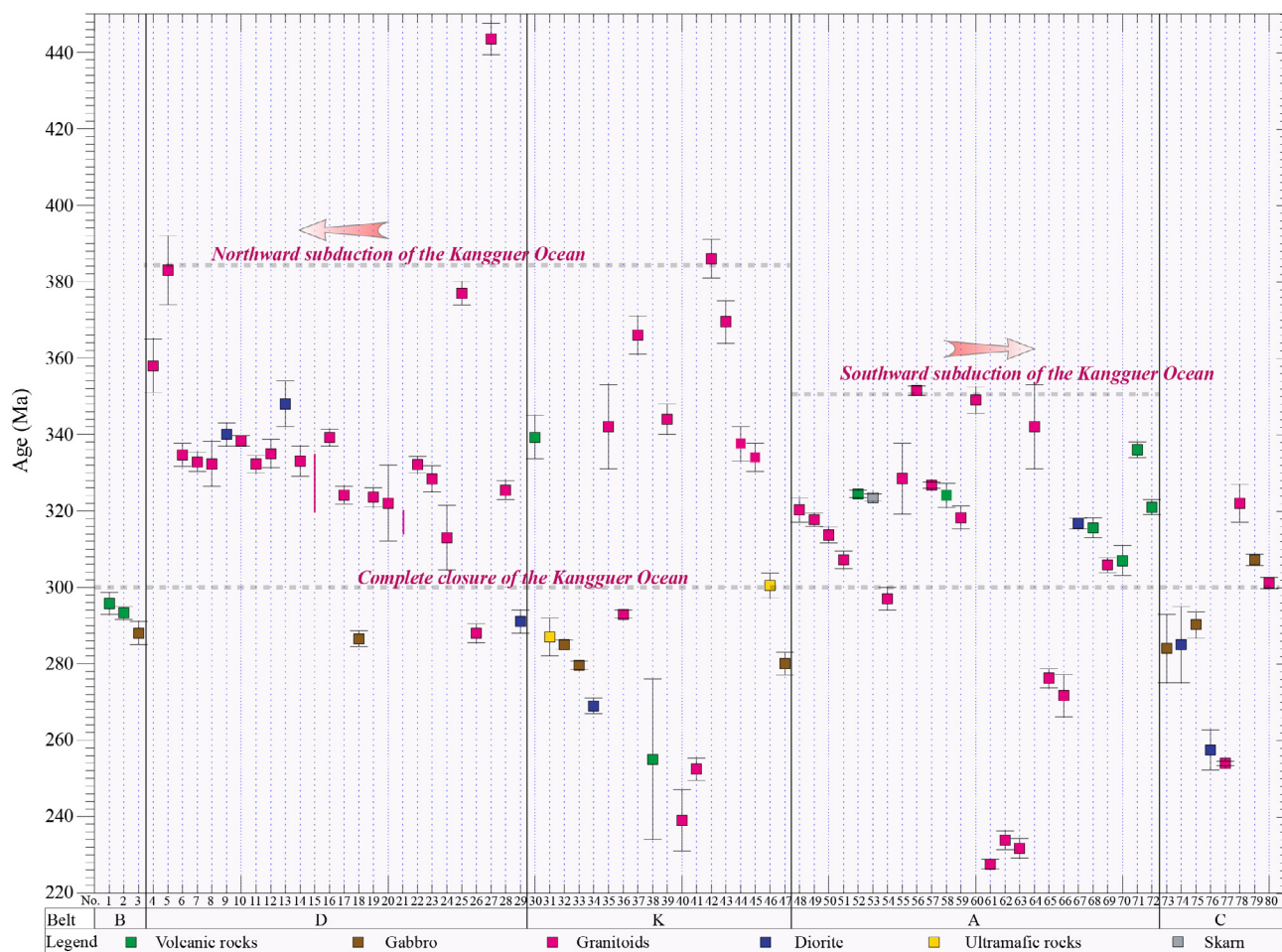


Fig. 8. Synthetic diagram showing all the published magmatic ages in the Eastern Tianshan. The number on the x-axis correspond to the number of references in Supplementary Table A4. Abbreviations: B-Bogda-Haerlike belt, K-Kanggur shear zone, A-Aqishan-Yamansu belt, M-Central Tianshan.

We suggest that the Carboniferous Aqishan-Yamansu belt may have been a forearc basin (Fig. 9a, b). Main arguments for this are as below: (1) Kanggur shear zone is located to the north of the Central Tianshan massif, with the Aqishan-Yamansu belt in between, (2) the Central Tianshan massif was likely a detrital source for the Aqishan-Yamansu belt; and (3) the Kanggur Ocean may have subducted southward beneath the Central Tianshan massif (Fig. 2). The Yamansu Formation may have deposited during the forearc basin opening.

5.1.3. Late Carboniferous fore-arc basin inversion

The gabbro emplacement and magmatic Ni–Cu–Co sulfide mineralization in the Eastern Tianshan (298–282 Ma; Mao et al., 2008; Fig. 8), and the large-scale Kanggur ductile shear movement (biotite $^{40}\text{Ar}/^{39}\text{Ar}$ plateau: ca. 290–270 Ma; Sm–Nd isochron orogenic Au mineralization age: ca. 290 ± 7 Ma) indicate that the Kanggur Ocean was closed no later than late Early Permian (Zhang et al., 2003; Xiao et al., 2004; Zuo et al., 2006). Recently, Zhang et al. (2015) obtained metamorphic zircon rim ages of the gneisses at Yamansu (301.5 ± 2.9 Ma) and Shaquanzi (301.1 ± 2.2 Ma) on the northern margin of the Central Tianshan, and interpreted the metamorphism was related to the collision during the Kanggur Ocean closure (Zhang et al., 2015). The widespread magmatic Ni–Cu–Co sulfide mineralization in the Eastern Tianshan suggests that the region had entered post-collisional tectonics after the late Early Permian (Figs. 8 and 9). The upper member of the Tugutubulak Formation consists of purplish-gray andesite, and discontinuous volcaniclastic rocks as well as intercalated fragments of fossil plants (Fig. 2). Meanwhile, more mantle materials were involved to the formation of granitoids with the younging trend (Fig. 4e, f). The

tectonic evolution could be envisaged as: 1) During ca. 350–325 Ma, the southward subduction of the Kanggur Ocean initiated and the slab rollback may occur during the process, leading to extension and the formation of the Aqishan-Yamansu forearc basin. At the same time, lithosphere mantle would be enriched by slab-derived fluids as a result of slab dehydration and minor lithosphere mantle would remelt the lower continental crust, giving rise to the formation of the Yamansu volcanic rocks and few intrusions (Fig. 9a). 2) During ca. 325–300 Ma, with the ongoing subduction, the slab may undergo breakoff due to two opposing forces: a) increased gravitational pull causing the subducted slab to sink, especially after it went through eclogite facies metamorphism; b) After slab breakoff, positive buoyancy dominated and slab rebound occurred (Fig. 9b), supported by the decrease of Sr/Y from the early to late Carboniferous granitoids (Fig. 4d; Atherton and Petford, 1993). As a result, the subduction angle decreased and the fore-arc basin evolved from extension to compression and more lithospheric mantle would be involved during the melting of lower continental crust/former mafic rocks, leading to the formation of the Tugutubulak Formation and large amounts intermediate-felsic intrusions such as the Bailingshan complex (Fig. 9b).

5.2. Genesis of the Aqishan-Yamansu Fe (-Cu) mineralization

Many features of the Aqishan-Yamansu Fe (-Cu) deposits resemble typical skarn deposits, such as the common occurrence of prograde skarn minerals (e.g., garnet and pyroxene) and the magmatic-hydrothermal origin for the Fe ore fluids (Jiang et al., 2016; Zhang et al., 2016a,b; Zhang et al., 2017). However, the clear absence of spatial

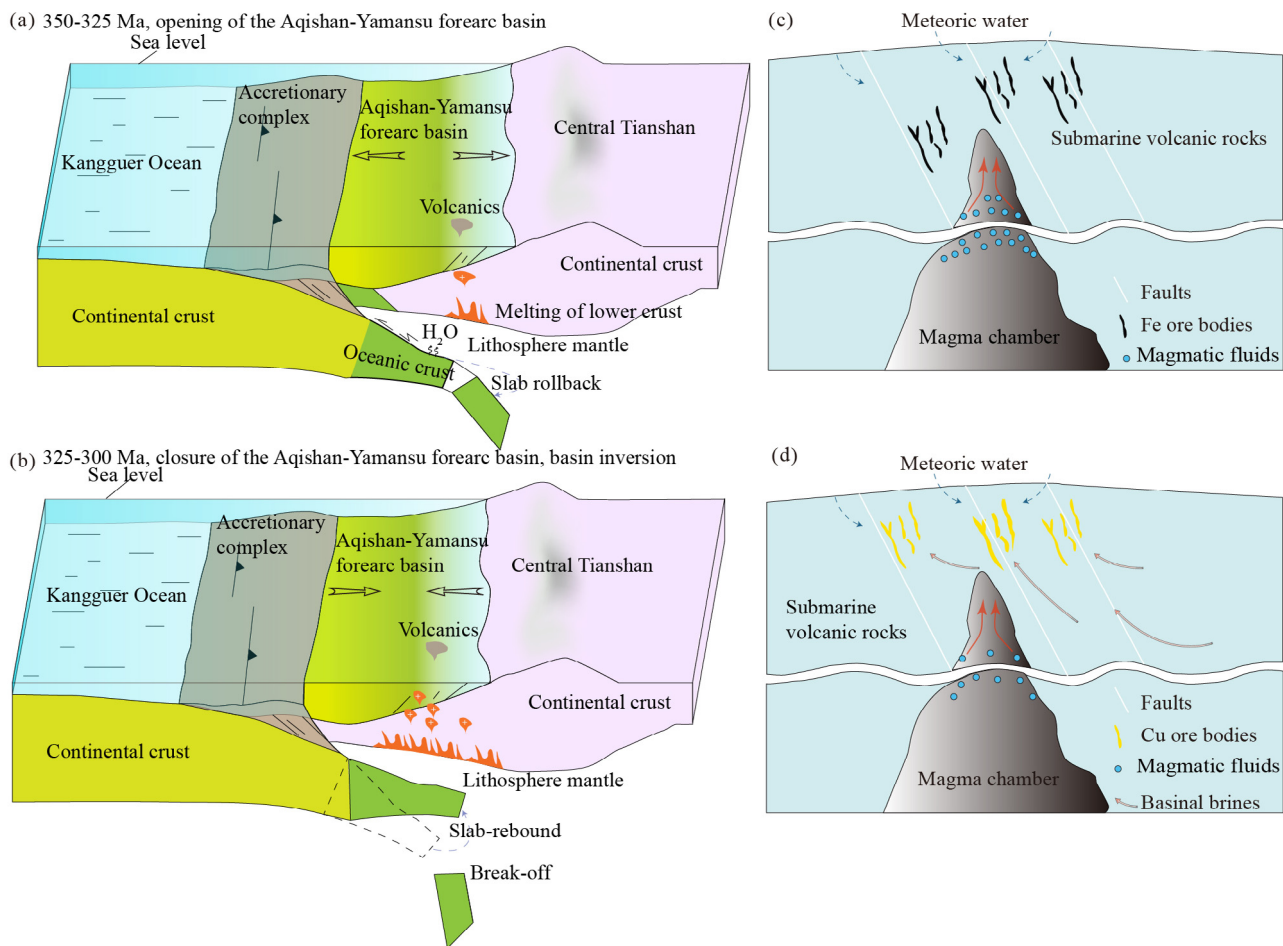


Fig. 9. (a), (b) Schematic model for the tectonic evolution of the Aqishan-Yamansu forearc basin during its (a) opening and (b) closure; (c), (d) Schematic metallogenetic model for the Late Carboniferous Aqishan-Yamansu Fe (-Cu) mineralization.

association with intrusive rocks and the involvement of seawater/basinal brine for the Cu mineralization are unlike typical skarn deposits (Meinert et al., 2005).

As mentioned before, the elevated $\delta^{34}\text{S}$ values in the Aqishan-Yamansu Cu mineralization stage may suggest the involvement of evaporite-sourced fluids and/or Carboniferous seawater or basinal brine, as supported also by the high salinities and low temperatures of the Cu ore fluids (Fig. 6). Based on the above discussion, we proposed a modified tectono-metallogenetic model for the Carboniferous Aqishan-Yamansu Fe (-Cu) mineralization. In the Early Carboniferous (ca. 350–325 Ma), the Aqishan-Yamansu belt may have been a forearc basin formed in a continental arc system (Fig. 9a). The Yamansu Formation were deposited and the Yamansu and Hongyuntan Fe mineralization occurred at the later stage of the forearc basin opening. With continued subduction of the Kanggūer Ocean, basin inversion (ca. 325–300 Ma) occurred along with intensive Fe-Cu mineralization (Fig. 9b). During the earlier Fe alteration/mineralization stage, magmatic-derived fluids may have migrated along the faults, reacted with the carbonate beds among the submarine volcanic ore host and formed the skarn-related Fe mineralization (Fig. 9c). Subsequently, the circulating hydrothermal fluids (with seawater/basinal brine input) may have leached sulfur from the host rocks to precipitate Cu sulfides, forming the superimposing (sub)-economic Cu mineralization (Fig. 9d).

External sulfur input has also been proposed in many major Cu-rich IOCG deposits (e.g. Benavides et al., 2007; Monteiro et al., 2008; Chen et al., 2011), and has likely led to the Cu mineralization in the Central Andean IOCG deposits (Chen, 2013). These Central Andean IOCG deposits were located in the Mesozoic continental margin rift basin, with

their peak mineralization coinciding with the basin inversion (Chen et al., 2013).

The probable external sulfur input (Chen, 2013, the absence of clear plutonic link (Williams et al., 2005; Zhao et al., 2016, 2017), as well as the peak mineralization coinciding temporally with the basin inversion (Chen et al., 2013) altogether suggest that the Paleozoic Aqishan-Yamansu Fe-Cu mineralization may have some similar features to the Central Andean IOCG deposits.

It is noteworthy that in some iron skarn mineralization, such as Daye, Handan-Xingtai district in eastern China, involvement of external sulfur could also be observed (Wen et al., 2017). In this kind deposits, iron skarn mineralization is closely related to the evaporite-bearing carbonate strata. The role of evaporite could be displayed by the following reaction $12\text{Fe}^{2+} + \text{SO}_4^{2-} + 12\text{H}_2\text{O} \rightleftharpoons 4\text{Fe}_3\text{O}_4 + \text{H}_2\text{S} + 22\text{H}^+$, which is important for the precipitation of magnetite. H^+ produced during the reaction could be neutralized by the surrounding carbonate rocks, driving the reaction continuously toward the right. This widespread evaporate within the carbonate host rocks could be viewed as a common feature of such iron skarn mineralization but its role is distinct from those described in Aqishan-Yamansu Fe (-Cu) belt in which external fluids were dominantly associated with Cu mineralization.

6. Conclusions

Detailed compilations of ore deposit geology, age, alteration/mineralization paragenesis and ore fluid geochemistry on the Carboniferous Aqishan-Yamansu Fe (-Cu) deposits show that:

- 1) The Carboniferous Aqishan-Yamansu belt was likely a forearc basin resulted from the south-dipping subduction of the Kangguer Ocean.
- 2) The Yamansu (Lower Carboniferous) and Tugutublak (upper Carboniferous) volcanic rocks were emplaced during the opening and closure of the Aqishan-Yamansu forearc basin, respectively.
- 3) Most of the Aqishan-Yamansu Fe (-Cu) deposits were formed during the late Carboniferous. The Fe mineralization was likely resulted from the interaction between deep-sourced magmatic fluids and submarine volcanic rocks, whilst the Cu mineralization may have related to the incursion of seawater/basin brines (external sulfur).
- 4) The probable external sulfur input, the absence of clear plutonic link, as well as the temporal coincidence of peak mineralization with basin inversion in the Aqishan-Yamansu Fe (-Cu) belt is comparable with the Mesozoic Central Andean IOCG belt.

Acknowledgements

The authors would like to thank the Editor-in-Chief and two anonymous reviewers. This study was financially supported by the Chinese National Science Fund for Distinguished Young Scholars (41725009) and Type-B Chinese academy of sciences strategic pilot science and technology special (XDB18030206). Juntao Yang is thanked for assisting with the field work. Discussion with Wanjian Lu has greatly improved the manuscript. We are grateful to the editor and three anonymous reviewers for their constructive comments. This is contribution No. IS-2622 from GIGCAS.

Appendix A. Supplementary data

Supplementary data to this article can be found online at <https://doi.org/10.1016/j.oregeorev.2018.12.012>.

References

- Atherton, M.P., Petford, N., 1993. Generation of sodium-rich magmas from newly underplated basaltic crust. *Nature* 362, 144–146.
- Benavides, J., Kyser, T.K., Clark, A.H., 2007. The Mantoverde Iron Oxide-Copper-Gold District, III Región, Chile: the role of regionally derived, nonmagmatic fluids in chalcopyrite mineralization. *Econ. Geol.* 102, 415–440.
- Chang, Z.S., Large, R.R., Maslenikov, V., 2008. Sulfur isotopes in sediment-hosted orogenic gold deposits: evidence for an early timing and a seawater sulfur source. *Geology* 36, 971–974.
- Charvet, J., Shu, L.S., Laurent-Charvet, S., 2007. Paleozoic structural and geodynamic evolution of eastern Tianshan (NW China): welding of the Tarim and Junggar plates. *Episodes* 30, 162–186.
- Chen, H.Y., 2013. External sulfur in IOCG mineralization: implications on definition and classification of the IOCG clan. *Ore Geol. Rev.* 51, 74–78.
- Chen, F.W., He, G.Q., Li, H.Q., 2003. Tectonic attribute of Qoltag orogenic belt in the Eastern Tianshan Mountains, northwestern China. *Geology in China* 30, 361–366 (in Chinese with English abstract).
- Chen, H.Y., Kyser, T.K., Clark, A.H., 2011. Contrasting fluids and reservoirs in the contiguous Marcona and Mina Justa iron oxide-Cu (-Ag-Au) deposits, south-central Peru. *Miner. Deposita* 46, 677–706.
- Chen, C.M., Lu, H.F., Jia, D., Cai, D.S., Wu, S.M., 1999. Closing history of the southern Tianshan oceanic basin, western China: an oblique collisional orogeny. *Tectonophysics* 302, 23–40.
- Chen, H.Y., Yang, J.T., Baker, M., 2012. Mineralization and fluid evolution of the Jiyuan polymetallic Cu–Ag–Pb–Zn–Au deposit, eastern Tianshan, NW China. *Int. Geol. Rev.* 54, 816–832.
- Chen, H.Y., Cooke, D.R., Baker, M.J., 2013. Mesozoic iron oxide copper-gold mineralization in the Central Andes and the Gondwana supercontinent breakup. *Econ. Geol.* 108, 37–44.
- Chi, G.X., Ni, P., 2007. Equations for calculation of NaCl/(NaCl + CaCl₂) ratios and salinities from hydrohalite-melting and ice-melting temperatures in the H₂O-NaCl-CaCl₂ system. *Acta Petrol. Sin.* 23, 33–37 (in Chinese with English abstract).
- Davis, D.W., Lowenstein, T.K., Spencer, R.J., 1990. Melting behavior of fluid inclusions in laboratory-grown halite crystals in the systems NaCl-H₂O, NaCl-KCl-H₂O, NaCl-MgCl₂-H₂O and NaCl-CaCl₂-H₂O. *Geochim. Cosmochim. Acta* 54, 591–601.
- Defant, M.J., Drummond, M.S., 1990. Derivation of some modern arc magmas by melting of young subducted lithosphere. *Nature* 347, 662–665.
- Dong, Y.P., Zhang, G.W., Neubauer, F., Liu, X., Hauzenberger, C., Zhou, D., Li, W., 2011. Syn- and post-collisional granitoids in the Central Tianshan orogen: geochemistry, geochronology and implications for tectonic evolution. *Gondwana Res.* 20, 568–581.
- Du, L., Long, X., Yuan, C., Zhang, Y., Huang, Z., Wang, X., Yang, Y., 2018. Mantle contribution and tectonic transition in the Aqishan-Yamansu Belt, Eastern Tianshan, NW China: insights from geochronology and geochemistry of Early Carboniferous to Early Permian felsic intrusions. *Lithos* 304–307, 230–244.
- Fan, W., Wang, Y., Zhang, A., Zhang, F., Zhang, Y., 2010. Permian arc-back-arc basin development along the Ailaoshan tectonic zone: geochemical, isotopic and geological evidence from the Mojiang volcanic rocks, Southwest China. *Lithos* 119, 553–568.
- Gao, J., Long, L., Klemd, R., Qian, Q., Liu, D., Xiong, X., Su, W., Liu, W., Wang, Y., Yang, F., 2009. Tectonic evolution of the South Tianshan orogen and adjacent regions, NW China: geochemical and age constraints of granitoid rocks. *Int. J. Earth Sci.* 98, 1221–1238.
- Han, B.F., He, G.Q., Wang, X.C., Guo, Z., 2011. Late Carboniferous collision between the Tarim and Kazakhstan-Yili terranes in the western segment of the South Tian Shan orogen, Central Asia, and implications for northern Xinjiang, western China. *Earth Sci. Rev.* 109, 74–93.
- Han, C.M., Xiao, W.J., Zhao, G.C., Mao, J.W., Li, S.Z., Yan, Z., Mao, Q.G., 2006. Major types, characteristics and geodynamic mechanism of Upper Paleozoic copper deposits in northern Xinjiang, northwestern China. *Ore Geol. Rev.* 28, 308–328.
- Han, C.M., Xiao, W.J., Zhao, G.C., Su, B.X., Sakyi, P.A., Ao, S.J., Wan, B., Zhang, J., Zhang, Z.Y., 2014. Late Paleozoic metallogenesis and evolution of the East Tianshan Orogenic Belt (NW China, Central Asia Orogenic Belt). *Geol. Ore Deposits* 56, 493–512.
- He, Z.Y., Zhang, Z.M., Zong, K.Q., Xiang, H., Chen, X.J., Xia, M.J., 2014. Zircon U-Pb and Hf isotopic studies of the Xingxingxia Complex from Eastern Tianshan (NW China): significance to the reconstruction and tectonics of the southern Central Asian Orogenic Belt. *Lithos* 190–191, 485–499.
- Hoefs, J., 1997. Stable Isotope Geochemistry, 3rd ed. Springer-Verlag, Berlin, pp. 1–201.
- Hou, G.S., Tang, H.F., Liu, C.Q., Wang, Y.B., 2005. Geochronological and geochemical study on the wallrocks of Tuwu-Yandong porphyry copper deposits, eastern Tianshan Mountains. *Acta Petrol. Sin.* 21, 1729–1736 (in Chinese with English abstract).
- Hou, T., Zhang, Z.C., Pirajno, F., Santosh, M., Encarnacion, J., Liu, J., Zhao, Z.D., Zhang, L.J., 2014b. Geology, tectonic settings and iron ore metallogenesis associated with submarine volcanism in China: an overview. *Ore Geol. Rev.* 57, 498–517.
- Hou, T., Zhang, Z.C., Santosh, M., Encarnacion, J., Zhu, J., Luo, W.J., 2014a. Geochronology and geochemistry of submarine volcanic rocks in the Yamansu iron deposit, Eastern Tianshan Mountains, NW China: constraints on the metallogenesis. *Ore Geol. Rev.* 56, 487–502.
- Hu, A.Q., Zhang, G.X., Zhang, Q.F., Chen, Y.B., 1998. Constraints on the age of basement and crustal growth in Tianshan orogen by Nd isotopic composition. *Sci. China, Ser. D Earth Sci.* 41, 648–657.
- Huang, X.W., Qi, L., Meng, Y.M., 2013a. Trace element and REE geochemistry of minerals from Heifengshan, Shuangfengshan and Shaquanzi (Cu-) Fe deposits, eastern Tianshan Mountains. *Mineral Deposits* 32, 1188–1210 (in Chinese with English abstract).
- Huang, X.W., Qi, L., Gao, J.F., Zhou, M.F., 2013b. First reliable Re-Os ages of pyrite and stable isotope compositions of Fe(-Cu) deposits in the Hami Region, Eastern Tianshan Orogenic Belt, NW China. *Resour. Geol.* 53, 166–187.
- Huang, X.W., Qi, L., Wang, Y.C., Liu, Y.Y., 2014. Re-Os dating of magnetite from the Shaquanzi Fe-Cu deposit, eastern Tianshan, NW China. *Sci. China (Earth Sci.)* 57, 267–277.
- Huang, X.W., Zhou, M.F., Beaudoin, G., Gao, J.F., Qi, L., Lyu, C., 2018. Origin of the volcanic-hosted Yamansu Fe deposit, Eastern Tianshan, NW China: constraints from pyrite Re-Os isotopes, stable isotopes, and in situ magnetite trace elements. *Miner. Deposita* 81, 62. <https://doi.org/10.1007/s00126-018-0794-4>.
- Jiang, H.J., Han, J.S., Chen, H.Y., Zheng, Y., Zhang, W.F., Lu, W.J., Deng, G., Tan, Z.X., 2016. Hydrothermal alteration, fluid inclusions and stable isotope characteristics of the Shaquanzi Fe-Cu deposit, eastern Tianshan: implications for ore genesis and deposit type. *Ore Geol. Rev.* <https://doi.org/10.1016/j.oregeorev.2016.09.025>.
- Jiang, H.J., Han, J.S., Chen, H.Y., Zheng, Y., Lu, W.J., Deng, G., Tan, Z.X., 2017. An intra-continental back-arc basin setting for the Yamansu mineralization belt, eastern Tianshan: constraints from geochronology and geochemical study of the Shaquanzi igneous rocks. *Geosci. Front.* 8, 1447–1467.
- Khain, E.V., Bibikova, E.V., Salnikova, E.B., Kröner, A., Gibsher, A.S., Didenko, A.N., Degtyarev, K.E., Fedotova, A.A., 2003. The Palaeo-Asian ocean in the Neoproterozoic and early Palaeozoic: new geochronologic data and paleotectonic reconstructions. *Precambr. Res.* 122, 329–358.
- Klemd, R., John, T., Scherer, E.E., Rondenay, S., Gao, J., 2011. Changes in dip of subducted slabs at depth: petrological and geochronological evidence from HP-UHP rocks (Tianshan, NW-China). *Earth Planet. Sci. Lett.* 310, 9–20.
- Lei, R.X., Wu, C.Z., Zhang, Z.Z., Gu, L.X., Tang, J.H., Li, G., 2013. Geochronology, geochemistry and tectonic significances of the Yamansubei pluton in eastern Tianshan, Northwest China. *Acta Petrol. Sin.* 29, 2653–2664 (in Chinese with English abstract).
- Li, J.Y., 2004. Late Neoproterozoic and Paleozoic tectonic framework and evolution of eastern Xinjiang. *Geol. Rev.* 50, 304–322 (in Chinese with English abstract).
- Li, H.M., Ding, J.H., Li, L.X., Yao, T., 2014. The genesis of the skarn and the genetic type of the Yamansu iron deposits, Eastern Tianshan, Xinjiang. *Acta Geol. Sin.* 88, 2477–2489 (in Chinese with English abstract).
- Li, Q.G., Liu, S.W., Wang, Z.Q., Han, B.F., Shu, G.M., Wang, T., 2008a. Electron microprobe monazite geochronological constraints on the Late Paleozoic tectono-thermal evolution in the Chinese Tianshan. *J. Geol. Soc.* 165, 511–522.
- Li, W.Q., Ma, H.D., Wang, R., Wang, H., Xia, B., 2008b. SHRIMP dating and Nd-Sr isotopic tracing of Kanggurtaike ophiolite in eastern Tianshan, Xinjiang. *Acta Petrol. Sin.* 24, 773–780 (in Chinese with English abstract).
- Li, X.M., Xia, Z.C., Xu, X.Y., Ma, Z.P., Wang, L.S., 2005. Zircon U-Pb geochronology of volcanic rocks of the Qi'eshan Group in the East Tianshan Mountains. *Geol. Bull. China* 23, 1215–1220 (in Chinese with English abstract).
- Li, Y., Yang, J.S., Zhang, J., Li, T.F., Chen, S.Y., Ren, Y.F., Xu, X.Z., 2011. Tectonical

- significance of the Carboniferous volcanic rocks in eastern Tianshan. *Acta Petrol. Sin.* 27, 193–209 (in Chinese with English abstract).
- Liu, C., 2009. Volcanic Rocks around the Shiyigong Gold Mine, Shanshan and the Relationship to the Gold Mineralization. Master Thesis, Xinjiang University (in Chinese with English abstract).
- Liu, S.W., Guo, Z.J., Zhang, Z.C., Li, Q.G., Zheng, H.F., 2004. Nature of the Precambrian metamorphic blocks in the eastern segment of Central Tianshan: constraint from geochronology and Nd isotopic geochemistry. *Sci. China, Ser. D, Earth Sci.* 47, 1085–1094.
- Luo, T., Liao, Q.A., Chen, J.P., Zhang, X.H., Guo, D.B., Hu, Z.C., 2012. LA-ICP-MS zircon U-Pb dating of the volcanic rocks from Yamansu Formation in the Eastern Tianshan, and Its geological significance. *Earth Sci.-J. China Univ. Geosci.* 37, 1338–1352 (in Chinese with English abstract).
- Luo, T., Liao, Q.A., Zhang, X.H., Chen, J.P., Wang, G.C., Huang, X., 2015. Geochronology and geochemistry of Carboniferous metabasalts in eastern Tianshan, Central Asia: evidence of a back-arc basin. *Int. Geol. Rev.* 58, 756–772.
- Ma, X.X., Shu, L.S., Jahn, B.M., Zhu, W., Faure, M., 2012a. Precambrian tectonic evolution of Central Tianshan, NW China: constraints from U-Pb dating and in situ Hf isotopic analysis of detrital zircons. *Precambr. Res.* 222–223, 450–473.
- Ma, X.X., Shu, L.S., Santosh, M., Li, J., 2012b. Detrital zircon U-Pb geochronology and Hf isotope data from Central Tianshan suggesting a link with the Tarim Block: implications on Proterozoic supercontinent history. *Precambr. Res.* 206–207, 1–16.
- Mao, J.W., Goldfarb, R.J., Wang, Y.T., Hart, C.J., Wang, Z.L., Yang, J.M., 2005. Late Paleozoic base and precious metal deposits, East Tianshan, Xinjiang, China: characteristics and geodynamic setting. *Episodes* 28, 23–35.
- Mao, J.W., Pirajno, F., Zhang, Z.H., Chai, F.M., Wu, H., Chen, S.P., Cheng, L.S., Yang, J.M., Zhang, C.Q., 2008. A review of the Cu-Ni sulphide deposits in the Chinese Tianshan and Altay orogens (Xinjiang Autonomous Region, NW China): principal characteristics and ore-forming processes. *J. Asian Earth Sci.* 32, 184–203.
- Meinert, L.D., Dipple, G.M., Nicolsescu, S., 2005. World skarn deposits, Economic Geology 100th Anniversary Volume, pp. 299–336.
- Meschede, M., 1986. A method of discriminating between different types of midocean ridge basalts and continental tholeiites with the Nb-Zr-Y diagram. *Chem. Geol.* 56, 207–218.
- Monteiro, L.V.S., Xavier, R.P., de Carvalho, E.R., Hitzman, M.W., Johnson, C.A., de Souza, C.R., Torresi, I., 2008. Spatial and temporal zoning of hydrothermal alteration and mineralization in the Sossego iron oxide-copper-gold deposit, Carajás Mineral Province, Brazil: paragenesis and stable isotope constraints. *Mineral Deposita* 43, 129–159.
- Morishita, T., Dilek, Y., Shallot, M., Tamura, A., Arai, S., 2011. Insight into the uppermost mantle section of a maturing arc: the Eastern Mirdita ophiolite, Albania. *Lithos* 124, 215–226.
- Muhetaer, Z., Nijat, A., Wu, Z.N., 2015. Geochemical characteristics of the volcanics from the Southern Juelutou area and their constraints on the tectonic evolution of Paleo-Asian Ocean. *Earth Sci. Front.* 22, 238–250 (in Chinese with English abstract).
- Ohmoto, H., Rye, R.O., 1979. Isotopes of sulfur and carbon. In: Barns, H.L. (Ed.), *Geochemistry of Hydrothermal ore Deposits*. Wiley Interscience, New York, pp. 509–567.
- Pearce, J.A., 1996. Sources and settings of granitic rocks. *Episodes* 19, 120–125.
- Pearce, J.A., 2008. Geochemical fingerprinting of oceanic basalts with applications to ophiolite classification and the search for Archean oceanic crust. *Lithos* 100, 14–48.
- Pearce, J.A., Harris, N.B.W., Tindle, A.G., 1984. Trace-element discrimination diagrams for the tectonic interpretation of granitic-rocks. *J. Petrol.* 25, 956–983.
- Pirajno, F., 2013. The Geology and Tectonic Settings of China's Mineral Deposits. Springer Science and Business Media, pp. 1–679.
- Pirajno, F., Mao, J.W., Zhang, Z.C., Zhang, Z.H., Chai, F.M., 2008. The association of mafic-ultramafic intrusions and A-type magmatism in the Tian Shan and Altay orogens, NW China: implications for geodynamic evolution and potential for the discovery of new ore deposits. *J. Asian Earth Sci.* 32, 165–183.
- Qin, K.Z., Fang, T.H., Wang, S.L., Zhu, B.Q., Feng, Y.M., Yu, H.F., Xiu, Q.Y., 2002. Plate tectonics division, evolution and metallogenetic setting in eastern Tianshan mountains, NE-China. *Xinjiang Geol.* 20, 302–308 (in Chinese with English abstract).
- Reagan, M.K., Ishizuka, O., Stern, R.J., Kelley, K.A., Ohara, Y., Blichert-Toft, J., Bloomer, S.H., Cash, J., Fryer, P., Hanan, B.B., 2010. Fore-arc basalts and subduction initiation in the Izu-Bonin-Mariana system. *Geochim. Geophys. Geosyst.* 11.
- Sang, S.J., Peng, M.X., Guo, Y.H., 2003. Optimized Target Areas and Evaluation Report of Resource in the Caixiahan to Jintian area. Xinjiang Institute of Geological Investigation, pp. 42–44 (in Chinese).
- Shuto, K., Ishimoto, H., Hirahara, Y., Sato, M., Matsui, K., Fujibayashi, N., Takazawa, E., Yabuki, K., Sekine, M., Kato, M., 2006. Geochemical secular variation of magma source during Early to Middle Miocene time in the Niigata area, NE Japan: asthenospheric mantle upwelling during back-arc basin opening. *Lithos* 86, 1–33.
- Su, C.Q., Jiang, C.Y., Xia, M.Z., Wei, W., Pan, R., 2009. Geochemistry and zircons SHRIMP U-Pb age of volcanic rocks of Aqishan Formation in the eastern area of north Tianshan, China. *Acta Petrol. Sin.* 25, 901–915 (in Chinese with English abstract).
- Su, B.X., Qin, K.Z., Sakyi, P.A., Li, X.H., Yang, Y.H., Sun, H., Tang, D.M., Liu, P.P., Xiao, Q.H., Malaviarachchi, S.P.K., 2011. U-Pb ages and Hf-O isotopes of zircons from Late Paleozoic mafic-ultramafic units in the southern Central Asian Orogenic Belt: tectonic implications and evidence for an Early-Permian mantle plume. *Gondwana Res.* 20, 516–531.
- Su, B.X., Qin, K.Z., Tang, D.M., Sakyi, P.A., Liu, P.P., Sun, H., Xiao, Q.H., 2013. Late Paleozoic mafic-ultramafic intrusions in southern Central Asian Orogenic Belt (NW China): insight into magmatic Ni-Cu sulfide mineralization in orogenic setting. *Ore Geol. Rev.* 51, 57–73.
- Thode, H.G., 1991. Sulphur isotopes in nature and the environment: an overview. In: Krouse, H.R., Grinenko, V.A. (Eds.), *Stable Isotopes: Natural and Anthropogenic* Sulfur 1013 in the Environment. Scope. John Wiley, New York, pp. 1–26.
- Wang, B., Cluzel, D., Jahn, B.M., Shu, L.S., Chen, Y., Zhai, Y.Z., Branquet, Y., Barbanson, L., Sizaret, S., 2014. Late Paleozoic pre- and syn-kinematic plutons of the Kanggur-Huangshan Shear Zone: inference on the tectonic evolution of the eastern Chinese Tianshan. *Am. J. Sci.* 314, 43–79.
- Wang, L.S., Li, H.Q., Chen, Y.C., Liu, D.Q., 2005. Geological feature and mineralization epoch of Bailingshan iron deposit, Hami, Xinjiang, China. *Mineral Deposits* 24, 264–269 (in Chinese with English abstract).
- Wang, J.B., Wang, Y.W., He, Z.J., 2006. Ore deposits as a guide to the tectonic evolution in the East Tianshan Mountains, NW China. *Geol. China* 33, 461–469 (in Chinese with English abstract).
- Wang, W., Xia, F., Chai, F.M., Wu, S.J., Li, Q., Geng, X.X., Meng, Q.P., 2016. Geochronology and geochemistry of volcanic rocks from the Yamansu Formation in eastern Tianshan Mountains and their tectonic implications. *Acta Petrol. Mineral.* 35, 768–790 (in Chinese with English abstract).
- Wang, Y.H., Xue, C.J., Liu, J.J., Wang, J.P., Yang, J.T., Zhang, F.F., Zhao, Z.N., Zhao, Y.J., Liu, B., 2015. Early Carboniferous adakitic rocks in the area of the Tuwu deposit, eastern Tianshan, NW China: slab melting and implications for porphyry copper mineralization. *J. Asian Earth Sci.* 103, 332–349.
- Wen, G., Bi, S.J., Li, J.W., 2017. Role of evaporitic sulfates in iron skarn mineralization: a fluid inclusion and sulfur isotope study from the Xishimen deposit, Handan-Xingtai district, North China Craton. *Miner. Deposita* 52, 495–514.
- Williams, P.J., Barton, M.D., Johnson, D.A., Fontboté, L., Halter, A.D., Mark, G., Oliver, N. H.S., Marschik, R., 2005. Iron-oxide copper-gold deposits: geology, space-time distribution, and possible modes of origin. *Economic Geology* 100th Anniversary Volume, pp. 371–405.
- Windley, B.F., Alexeev, D., Xiao, W.J., Kröner, A., Badarch, G., 2007. Tectonic models for accretion of the Central Asian Orogenic Belt. *J. Geol. Soc.* 164, 31–47.
- Woodhead, J.D., Hergt, J.M., Davidson, J.P., Egging, S.M., 2001. Hafnium isotope evidence for 'conservative' element mobility during subduction zone process. *Earth Planet. Sci. Lett.* 192, 331–346.
- Wu, C.Z., Zhang, Z.Z., Zaw, K., Della-Pasqua, F., Tang, J.H., Zheng, Y.C., San, J.Z., 2006. Geochronology, geochemistry and tectonic significances of the Hongyuntan granitoids in the Juelutou area, Eastern Tianshan. *Acta Petrol. Sin.* 22, 1121–1134 (in Chinese with English abstract).
- Xiao, B., Chen, H.Y., Hollings, P., Han, J.S., Wang, Y.F., Yang, J.T., Cai, K.D., 2017. Magmatic evolution of the Tuwu-Yandong porphyry Cu belt, NW China: constraints from geochronology, geochemistry and Sr-Nd-Hf isotopes. *Gondwana Res.* 43, 74–91.
- Xiao, W.J., Zhang, L.C., Qin, K.Z., Sun, S., Li, J.L., 2004. Paleozoic accretionary and collisional tectonics of the eastern Tianshan (China): implications for the continental growth of central Asia. *Am. J. Sci.* 304, 370–395.
- Xiao, W.J., Li, S.Z., Santosh, M., Jahn, B.M., 2012. Orogenic belts in Central Asia: correlations and connections. *J. Asian Earth Sci.* 49, 1–6.
- Xiao, W.J., Windley, B.F., Allen, M.B., Han, C.M., 2013. Paleozoic multiple accretionary and collisional tectonics of the Chinese Tianshan orogenic collage. *Gondwana Res.* 23, 1316–1341.
- Xiao, W.J., Windley, B.F., Sun, S., Li, J.L., Huang, B.C., Han, C.M., Yuan, C., Sun, M., Chen, H.L., 2015. A tale of amalgamation of three Permo-Triassic collage systems in Central Asia: oroclines, sutures, and terminal accretion. *Annu. Rev. Earth Planet. Sci.* 43, 477–507.
- Xu, L.L., Chai, F.M., Li, Q., Zeng, H., Geng, X.X., Xia, F., Deng, G., 2014. Geochemistry and zircon U-Pb age of volcanic rocks from the Shaquanzi Fe-Cu deposit in East Tianshan Mountains and their geological significance. *Geol. China* 41, 1771–1790 (in Chinese with English abstract).
- Xu, X.W., Ma, T.L., Sun, L.Q., Cai, X.P., 2003. Characteristics and dynamic origin of the large-scale Juelutou ductile compressional zone in the eastern Tianshan Mountains, China. *J. Struct. Geol.* 25, 1901–1915.
- Xu, S.Q., Zhao, T.Y., Feng, J., Gao, Y.F., Tian, J.T., Yang, Z.F., Liu, D.Q., 2011. Study on regional metallogenetic regularity of marine volcanic type iron ore in the East Tianshan of Xinjiang. *Xinjiang Geol.* 29, 173–177 (in Chinese with English abstract).
- Zhang, W.F., Chen, H.Y., Han, J.S., Zhao, L.D., Huang, J.H., Yang, J.T., Yan, X.L., 2016a. Geochronology and geochemistry of igneous rocks in the Bailingshan area: implications for the tectonic setting of late Paleozoic magmatism and iron skarn mineralization in the eastern Tianshan, NW China. *Gondwana Res.* 38, 40–59.
- Zhang, W.F., Chen, H.Y., Peng, L.H., Zhao, L.D., Lu, W.J., Zhang, Z.J., Yang, J.T., Sun, J., 2017. Ore genesis of the Duotoushan Fe-Cu deposit, Eastern Tianshan, NW China: constraints from ore geology, mineral geochemistry, fluid inclusion and stable isotopes. *Ore Geol. Rev.* <https://doi.org/10.1016/j.oregeorev.2017.02.021>.
- Zhang, X.H., Huang, X., Chen, J.P., Liao, Q.A., Duan, X.F., 2012b. Stratigraphical Sequence of Carboniferous Marine Volcanic-Deposit Rock and Its Geological Age in Juelutou Area, Eastern Tianshan. *Earth Sci.-J. China Univ. Geosci.* 37, 1305–1314 (in Chinese with English abstract).
- Zhang, L.C., Shen, Y.C., Ji, J.S., 2003. Characteristics and genesis of Kanggur gold deposit in the eastern Tianshan mountains, NW China: evidence from geology, isotope distribution and chronology. *Ore Geol. Rev.* 23, 71–90.
- Zhang, Y.Y., Sun, M., Yuan, C., Long, X.P., Jiang, Y.D., Li, P.F., Huang, Z.Y., Du, L., 2018. Alternating trench advance and retreat: insights from Paleozoic Magmatism in the Eastern Tianshan, Central Asian Orogenic Belt. *Tectonics* 37, 2142–2164.
- Zhang, L.C., Wang, Y.T., Chen, X.F., Ma, S.Q., Wang, Z.H., Yu, C.F., 2013. Mineralogy, mineral chemistry and genesis of the Hongyuntan iron deposit in East Tianshan Mountains, Xinjiang. *Acta Petrol. Mineral.* 32, 431–449 (in Chinese with English abstract).
- Zhang, X.R., Zhao, G.C., Eizenhöfer, P.R., Sun, M., Han, Y.G., Hou, W.Z., Liu, D.X., Wang, B., Liu, Q., Xu, B., 2015. Paleozoic magmatism and metamorphism in the Central Tianshan Block revealed by U-Pb and Lu-Hf isotope studies of detrital zircons from

- the South Tianshan belt, NW China. *Lithos* 233, 193–208.
- Zhang, X.R., Zhao, G.C., Sun, M., Eizenhöfer, P.R., Han, Y., Hou, W., Liu, D., Wang, B., Liu, Q., Xu, B., 2016b. Tectonic evolution from subduction to arc-continent collision of the Junggar ocean: constraints from U-Pb dating and Hf isotopes of detrital zircons from the North Tianshan belt, NW China. *Geol. Soc. Am. Bull.* 128, 644–660.
- Zhang, D.Y., Zhou, T.F., Yuan, F., Liu, S., Lu, Y.J., Xu, C., Ning, F.Q., 2012a. Geochronology and geological indication of the native copper mineralized basalt formation in Jueluotage area, Eastern Tianshan, Xinjiang. *Acta Petrol. Sin.* 28, 2392–2400 (in Chinese with English abstract).
- Zhao, L.D., Chen, H.Y., Zhang, L., Li, D.F., Zhang, W.F., Wang, C.M., Yang, J.T., Yan, X.L., 2016. Magnetite geochemistry of the Heijianshan Fe–Cu (–Au) deposit in Eastern Tianshan: metallogenetic implications for submarine volcanic-hosted Fe–Cu deposits in NW China. *Ore Geol. Rev.* <https://doi.org/10.1016/j.oregeorev.2016.07.022>.
- Zhao, L.D., Chen, H.Y., Zhang, L., Xia, X., Zhang, W.F., Li, D.F., Lu, W.J., Liang, P., Li, R., Yang, J.T., Yan, X.L., 2017. Geology and ore genesis of the late Paleozoic Heijianshan Fe oxide–Cu (–Au) deposit in the Eastern Tianshan, NW China. *Ore Geol. Rev.* 91, 110–132.
- Zhao, L.D., Chen, H.Y., Zhang, L., Zhang, W.F., Yang, J.T., Yan, X.L., 2018. The Late Paleozoic magmatic evolution of the Aqishan-Yamansu belt, Eastern Tianshan: constraints from geochronology, geochemistry and Sr–Nd–Pb–Hf isotopes of igneous rocks. *J. Asian Earth Sci.* 153, 170–192. <https://doi.org/10.1016/j.jseas.2017.07.038>.
- Zheng, R.Q., 2015. Geological characteristics and genesis of Hongyuntan iron deposits in the Eastern Tianshan, Xinjiang. Master Thesis, China University of Geoscience (Beijing) 1–102 (in Chinese with English abstract).
- Zhou, T.F., Yuan, F., Zhang, D.Y., Fan, Y., Liu, S., Peng, M.X., Zhang, J.D., 2010. Geochronology, tectonic setting and mineralization of granitoids in Jueluotage area, eastern Tianshan, Xingjiang. *Acta Petrol. Sin.* 26, 478–502 (in Chinese with English abstract).
- Zong, K.Q., Zhang, Z.M., He, Z.Y., Hu, Z.C., Santosh, M., Liu, Y.S., Wang, W., 2012. Early Paleozoic high-pressure granulites from the Dunhuang block, northeastern Tarim Craton: constraints on continental collision in the southern Central Asian Orogenic Belt. *J. Metamorph. Geol.* 30, 753–768.
- Zuo, G.C., Liang, G.L., Chen, J., Gao, J.B., Xing, D.C., Li, S.X., 2006. Late Paleozoic tectonic framework and evolution in the Jiabaishan area, Qoltag, eastern Tianshan Mountains, Northwestern China. *Geol. Bull. China* 25, 48–57 (in Chinese with English abstract).